Supporting Information

Biocompatible pure organic porous nanocage for enhanced photodynamic therapy

Zhong-Hong Zhu,[a,†] Di Zhang,[a,†] Jian Chen,[b] Hua-Hong Zou,[c] Zhiqiang Ni,[a] Yutong Yang,[a] Yating Hu,[d,*] Ruiyuan Liu,[b,*] Guangxue Feng,[a,*] and Ben Zhong Tang[e]

[a] State Key Laboratory of Luminescent Materials and Devices, Guangdong Provincial Key Laboratory of Luminescence from Molecular Aggregates, School of Materials Science and Engineering, South China University of Technology, Guangzhou, 510640, China

*E-mail: fenggx@scut.edu.cn (G. Feng)

[b] Guangdong Provincial Key Laboratory of Medical Image Processing, School of Biomedical Engineering, Southern Medical University, Guangzhou, 510515, China

*E-mail: ruiyliu@smu.edu.cn (R. Liu)

[c] School of Chemistry and Pharmaceutical Sciences, State Key Laboratory for Chemistry and Molecular Engineering of Medicinal Resources, Guangxi Normal University, Guilin 541004, P. R. China

[d] Guangzhou Key Laboratory of Low-Dimensional Materials and Energy Storage Devices, School of Materials and Energy, Guangdong University of Technology, Guangzhou 510006, China

*E-mail: yatinghu@gdut.edu.cn (Y. Hu)

[e] Shenzhen Institute of Aggregate Science and Engineering, School of Science and Engineering, The Chinese University of Hong Kong, Shenzhen 518172, China

Table of Contents:

	(20 mW·cm^{-2}) in mixture solvent H_2O/DMSO (V_{water}/V_{DMSO} = 99:1).
Figure S15	Comparison of photocurrent signals and electrochemical impedance spectroscopy (EIS) of PyTtDy, PyTtDy-CH_3I and Py-Cage.
Figure S16	Electron paramagnetic resonance (EPR) spectra of DMPO−·O_2^-, DMPO−·OH and TEMP−$^1O_2$ for Py-Cage (a), PyTtDy-CH_3I (b) and PyTtDy (c) before and after light irradiation.
Figure S17	Fluorescence (PL) spectra (a) and intensity changes at 662 nm (b) of Ce6 aqueous solutions with different concentrations.
Figure S18	Absorption spectrum changes of ABDA (20 μM) in the presence of Py-Cage (a) and Ce6 (b) in mixture solvent H_2O/DMSO (V_{water}/V_{DMSO} = 99:1) under the irradiation (20 mW·cm^{-2}) with different duration in an oxygen environment.
Figure S19	Fluorescence spectrum changes of DCFH (50 μM) containing different concentrations of Ce6 (a-c, 10 μg/mL-20 μg/mL) and Py-Cage (d-f, 10 μg/mL-20 μg/mL), respectively, and under light irradiation conditions (20 mW·cm^{-2}).
Figure S20	Comparison of fluorescence changes (I / I_0) of DCFH with different concentrations of Ce6 and Py-Cage under light irradiation.
Figure S21	The dihydroethidium (DHE) probe was used to detect the production of ·O_2^- after co-incubation of Py-Cage (40 μg/mL) with 4T1 cancer cells and under white light irradiation (60 mW·cm^{-2}), and the red fluorescence was the fluorescein produced by DHE in response to ·O_2^-.
Figure S22	Live/dead cell staining of 4T1 cells co-incubated assays after different treatment, live cells were stained green by CAM and dead cells were stained red by PI. Scale bar = 100 μm.
Figure S23	(a) Fluorescence images of tumor bearing mice at different times after Py-Cage injection (300 μg/mL, 100 μL); (b) Py-Cage distribution in mouse major organs and tumors collected at 48 h post injection.
Figure S24	Fluorescence images of healthy mice at different times after Py-Cage injection through tail vein, and the ex vivo fluorescence imaging of various vital organs of mice at 72 h post injection.
Figure S25	Blood routine parameters (white blood cells (WBC and MON), lymphocytes (LYMPH), neutrophils (GRAN), red blood cells (RBC), hematocrit (HCT), hemoglobin (HGB), mean muscle tone (MCV), erythrocyte hemoglobin content (MCH), erythrocyte distribution width (RDW), platelet volume (MPV) and platelet volume distribution width (PDW)) of normal mice injected with PBS or Py-Cage, respectively. Data presented mean ± SD, n = 3, No significant difference.
Figure S26	H&E staining images of major organ sections of normal mice treated with PBS or Py-Cage. Scale bar = 100 μm.
Figure S27	Some important blood routine parameters (red blood cells (RBC), hematocrit (HCT), mean muscle tone (MCV), erythrocyte hemoglobin content (MCH), erythrocyte distribution width (RDW), hemoglobin (HGB), Platelet volume (MPV) and platelet volume distribution width (PDW)) of healthy rats injected with PBS or Py-Cage, respectively. Data presented mean ± SD, n = 3, No significant difference.
Figure S28	Some important blood biochemical parameters (low-density lipoprotein (LDL), triglyceride (TG), high-density lipoprotein cholesterol (HDL), glucose (GLU)) of healthy rats injected with PBS or Py-Cage, respectively. Data presented mean ± SD, n = 3, No significant difference.
Figure S29	(a and b) TEM images of Py-Cage NPs. Comparison of UV-Vis absorption spectra (c) and fluorescence spectra (d) of Py-Cage and Py-Cage NPs under the same

	concentration conditions (10 μg/mL).
Figure S30	(a) The PL spectrum changes of DCFH (50 μM) in the presence of Py-Cage NPs (10 μg/mL) upon light irradiation (20 $mW \cdot cm^{-2}$) in H_2O; (b) the ROS production of Py-Cage, Py-Cage NPs (10 μg/mL) under white light irradiation (white light, 20 $mW \cdot cm^{-2}$) using DCFH as an indicator; (c) absorption spectrum changes of ABDA (20 μM) in the presence of Py-Cage NPs in H_2O under the irradiation (20 $mW \cdot cm^{-2}$) with different duration; (d and e) the $^1O_2$ production of Py-Cage and Py-Cage NPs under white light irradiation (20 $mW \cdot cm^{-2}$) using ABDA as an indicator; (f) the PL spectrum changes of DHR123 (20 μM) in the presence of Py-Cage NPs (10 μg/mL) upon light irradiation (20 $mW \cdot cm^{-2}$) in H_2O; (g) The $\cdot O_2^-$ production of Py-Cage, Py-Cage NPs (10 μg/mL) under white light irradiation (white light, 20 $mW \cdot cm^{-2}$) using DHR123 as an indicator; (h) the PL spectrum changes of HPF (20 μM) in the presence of Py-Cage NPs (10 μg/mL) upon light irradiation (20 $mW \cdot cm^{-2}$) in H_2O; (i) the ·OH production of Py-Cage, Py-Cage NPs (10 μg/mL) under white light irradiation (white light, 20 $mW \cdot cm^{-2}$) using HPF as an indicator.
Figure S31	Cell viabilities of 4T1 cells receiving different concentrations of Py-Cage NPs under (a) dark and (b) light conditions (80 $mW \cdot cm^{-2}$, 15 min).
Figure S32	Live/dead cell staining of 4T1 cells after different treatments, live cells were stained green by CAM and dead cells were stained red by PI. Scale bar = 200 μm.
Figure S33	Fluorescence images of tumor bearing mice at different times after intravenous injection of Py-Cage NPs (300 μg/mL, 100 μL/mouse) via tail vein.

Experimental Section

Materials and Measurements.

All reagents were obtained from commercial sources and used without further purification. Fourier transform infrared spectroscopy were recorded by transmission through KBr pellets containing *ca.* 0.5% of the Py-Cage using a PE Spectrum FT-IR spectrometer (400-4,000 cm^{-1}). Thermogravimetric analyses (TGA) were conducted in a flow of nitrogen at a heating rate of 5 °C/min using a NETZSCH TG 209 F3. Powder X-ray diffraction (PXRD) spectra were recorded on either a D8 Advance (Bruker) diffractometer at 293 K (Cu-Kα). The samples were prepared by crushing crystals and the powder placed on a grooved aluminum plate. Diffraction patterns were recorded from 2º to 55º at a rate of 5º min^{-1}. Ultraviolet-visible absorption spectra were recorded on a Shimadzu UV-2600 spectrophotometer, and fluorescence spectra were recorded on a Horiba Fluoromax-4 and FLS980 fluorescence spectrophotometer. The nitrogen adsorption and desorption of Py-Cage was tested by ASAP 2460 from Micromeritics. The EPR of Py-Cage was tested by Bruker A300 instrument in Germany. Dynamic light scattering with Malvern Zetasizer Nano-S90 was used to determine the hydrodynamic diameters of Py-Cage nanoparticles. Transmission electron microscope (TEM, JEM-2100F) was used to study Py-Cage organic nanocage. Confocal laser scanning microscope (CLSM) characterization was conducted with a confocal laser scanning microscope (Nikon A1, Japan). CCK-8 testing of photosensitizers was performed using Biotek ELX80 from Thermo Fisher Scientific. Flow testing of photosensitizers was performed using a BD LSRFortessa X-20 flow cytometer.

Synthesis of Py-Cage and PyTtDy-CH_3I.

Py-Cage: 768.42 mg 4,4',4",4"'-(porphyrin-5,10,15,20-tetrayl)tetrakis(*N*,*N*-dimethylaniline) (CAS: 14945-24-5, Bidepharm, China) (1 mmoL, PyTtDy) and 675.86 mg 4,4'-bis(bromomethyl)-1,1'-biphenyl (2 mmoL) was dissolved in excess 200 mL *N*,*N*-dimethylformamide (DMF) and refluxed at 160 °C for three days to obtain a dark green powder. The dark green powder was washed three times with DMF, followed by three washes with acetonitrile, and finally three times with ether, and then dried in a vacuum drying oven for 7 days to obtain Py-Cage (the yield is about 15%, based on PyTtDy). The composition of Py-Cage was determined by HRESI-MS, FTIR and NMR.

PyTtDy-CH_3I: 768.42 mg PyTtDy (1 mmoL) and 1.4194 g iodomethane (10 mmoL) was dissolved in excess 200 mL DMF and refluxed at 100 °C for 12 h to obtain a grey black powder. The grey black powder was washed three times with DMF, followed by three washes with acetonitrile, and finally three times with ether, and then dried in a vacuum drying oven for 7 days to obtain PyTtDy-CH_3I (the yield is about 75%, based on PyTtDy).[1-4] The composition of PyTtDy-CH_3I was determined by HRESI-MS and NMR.

ROS detection. 2',7'-Dichlorodihydrofluorescein diacetate (DCFH-DA) after activation with sodium hydroxide is used as a general ROS indicator.[5] The detailed steps are as follows: to the aqueous solution containing 50 μM DCFH, 10 μL of Py-Cage solution (1 mg/mL, in DMSO) was added to reach a final concentration of 10 μg/mL. After the above solution is irradiated with a xenon lamp white light (20 $mW \cdot cm^{-2}$, 3.2 $J \cdot cm^{-2}$) for different periods of time, the change in the fluorescence signal of the indicator is monitored by a fluorescence spectrometer. The excitation wavelength is 480 nm, and the fluorescence intensity of DCFH at 525 nm is recorded to indicate ROS generation. The same procedures were also applied to PyTtDy-CH_3I and PyTtDy. A curve was drawn to compare the fluorescence changes of DCFH in different solutions, so as to obtain the difference in ROS generation capacity.

Singlet oxygen detection of ABDA. 9,10-Anthracenediyl-bis(methylene)-dimalonic acid (ABDA) is used to monitor $^1O_2$ production. The specific steps are as follows: Add photosensitizer samples solution (DMSO; Py-Cage, PyTtDy-CH_3I and PyTtDy; 10 μL) with a stock concentration of 1 mg/L to the aqueous solution containing 20 μM ABDA. After the above solution was irradiated with white light

emitted by a xenon lamp of 20 mW·cm^{-2} (6.0 J·cm^{-2}) for different periods of time, the change in the absorption signal of the indicator ABDA at 380 nm was monitored by an ultraviolet-visible spectrometer to monitor the generation of $^1O_2$.

Singlet oxygen detection of SOSG. Specific single oxygen sensor green (SOSG) is used as an indicator of $^1O_2$. The detailed steps are as follows: to the aqueous solution containing 20 μM SOSG, 10 μL of stock solution (Py-Cage, PyTtDy-CH_3I and PyTtDy, 1 mg/mL, in DMSO) was added to reach a final concentration of 10 μg/mL. After the above solution is irradiated with white light emitted by a xenon lamp of 20 mW·cm^{-2} (1.4 J·cm^{-2}) for different periods of time, the change in the fluorescence signal of the indicator is monitored by a fluorescence spectrometer. The excitation wavelength used is 480 nm, and the fluorescence intensity of SOSG at 525 nm is recorded to evaluate $^1O_2$ generation.

Superoxide anion radical (·O_2^-) detection. Dihydrorhodamine 123 (DHR123) is used as an indicator of ·O_2^-, which can be converted to rhodamine 123 in the presence of ·O_2^-. The detailed steps are as follows: to the aqueous solution containing 20 μM DHR123, 10 μL of photosensitizer stock solution (Py-Cage, PyTtDy-CH_3I and PyTtDy, 1 mg/mL, in DMSO) was added to reach a final concentration of 10 μg/mL. After the above solution is irradiated with white light emitted by a xenon lamp of 20 mW·cm^{-2} (1.4 J·cm^{-2}) for different periods of time, the change in the fluorescence signal of the indicator is monitored by a fluorescence spectrometer. The excitation wavelength used is 480 nm, and the fluorescence intensity of DHR123 at 525 nm is recorded to indicate superoxide anion radical generation.

Hydroxyl radical (·OH) detection. Hydroxyphenylfluorescein (HPF) is used to monitor ·OH production. The specific steps are as follows: to the aqueous solution containing 10 μM HPF, 10 μL of photosensitizer stock solution (Py-Cage, PyTtDy-CH_3I and PyTtDy, 1 mg/mL, in DMSO) was added to reach a final concentration of 10 μg/mL. After the above solution is irradiated with white light emitted by a xenon lamp of 20 mW·cm^{-2} (1.4 J·cm^{-2}) for different periods of time, the change in the fluorescence signal of the indicator is monitored by a fluorescence spectrometer. The excitation wavelength used was 480 nm, and the fluorescence intensity of HPF at 515 nm was recorded to indicate the ·OH generation.

ROS detection with electron paramagnetic resonance (EPR). DMPO was used as trapping agent for ·OH and ·O_2^-. TEMP was used as the trapping agent for $^1O_2$. The photosensitizer samples Py-Cage and PyTtDy were respectively dissolved in H_2O/DMSO (V_{water}/V_{DMSO} = 99:1) mixed solution. Trapping agents were dissolved in CH_3OH, which was further added into Py-Cage or PyTtDy aqueous solution to reach a final concentration of 50 μM and 20 μg/mL for trapping agent and photosensitizer samples, respectively. The EPR spectra of the mixtures were recorded before and after light irradiation (Xenon lamp, 280 ~ 800 nm, 10 min, 100 mW·cm^{-2}, 60 J·cm^{-2}). The electron paramagnetic resonance (EPR, Bruker A300) spectra were measured to evaluate ROS generation.[3]

Confocal imaging of Py-Cage.

4T1 cancer cells were cultured in a 20 mm glass bottom petri dish at 37 °C in a humidified environment containing 5% CO_2. After the cells grew to 70% confluence, culture medium was aspirated and the cells were washed with PBS for three times. 40 μg/mL Py-Cage organic nanocage containing DMEM (10% FBS) was then added to cell culture petri dish. After 6 h incubation, the culture medium was aspirated and the cells were washed with PBS for three times. The cells were then incubated with 1 μg/mL DAPI containing DMEM for 30 min. CLSM images were acquired after washing the cells with PBS buffer for three times.

Intracellular ROS detection.

For intracellular ROS detection, Py-Cage (40 μg/mL) labeled 4T1 cells were incubated with ROS indicator 2',7'-dichlorodihydrofluorescein diacetate (DCFH-DA) for 30 min, followed by white light (80 mW·cm^{-2}) exposure for 10 min (48 J·cm^{-2}). The post treatment cells were then imaged by CLSM

with excitation filter of 488 nm, and emission filter of 500-530 nm.[6,7] Using Dihydroethidium (DHE) fluorescence probe to further detect the O_2^- level in cells. 4T1 cells were seeded into laser confocal petri dishes at a density of 2 x 10^5 cells / dish. Six groups of PBS, PBS + L, Py-Cage, Py-Cage + L 10 min, Py-Cage + L 15 min and Py-Cage + L 20 min were set, and after overnight cell culture, the Py-Cage solution was diluted to 40 μg/mL with fresh culture medium and added to the Py-Cage, Py-Cage + L 10 min, Py-Cage + L 15min and Py-Cage + L 20 min groups. After the cells were continuously incubated for another 6 hours, the cells were incubated with DHE fluorescence probe for 30 min. The PBS + L, Py-Cage + L 10 min, Py-Cage + L 15 min and Py-Cage + L 20 min groups were irradiated with white light (60 mW·cm^{-2}) for different times, among which the PBS + L group was irradiated for 10 min. After washing with PBS, the cells were observed by CLSM. The red fluorescence from DHE was collected from 600 to 630 nm upon excitation at 532 nm.

Cytotoxicity evaluated by CCK-8 assay.

4T1 cells were seeded into 96-well plates at a density of 1 × 10^4 cells / well and incubated in DMEM medium supplemented with 10% FBS and 1% penicillin-streptomycin in an incubator with 5% CO_2 at 37 °C for 12 h incubation, the Py-Cage solution was diluted to different concentrations with cell culture medium and added to 96-well plates to replace the original culture medium. Cells were cultured for 6 h and wash the cells with PBS, and then continuously irradiated (80 mW·cm^{-2}) with/without (light/dark toxicity) white light for 10 min (48 J·cm^{-2}). The treated cells were washed with PBS and the viability of cells was measured by the CCK-8 kit. The absorbance at 450 nm was recorded on a microplate reader.

Live/dead cell staining.

4T1 cells were seeded into laser confocal petri dishes at a density of 2 × 10^5 cells / dish. Groups of PBS, PBS + L, Py-Cage, and Py-Cage + L were set, and after overnight incubation, the Py-Cage solution was diluted to 80 μg/mL with cell culture medium to be added to the Py-Cage and Py-Cage + L groups. Cells were incubated for 6 h and after various treatments (with/without 80 mW·cm^{-2} white light irradiation for 10 min, 48 J·cm^{-2}), 4T1 cells were incubated with a mixture of calcein acetoxymethyl ester (AM) (2 μg/mL) and propidium iodide (PI) (5 μg/mL) for further live/dead cells staining. After washing with PBS, the cells were observed by CLSM. The green fluorescence from AM was collected from 500 to 530 nm upon excitation at 488 nm, and the red fluorescence from PI was collected from 600 to 630 nm upon excitation at 532 nm.

Flow Cytometry Analysis.

4T1 cells were seeded on 6-well plates at a density of 2 × 10^5 cells / well and cultured overnight for cell adherence. Four groups of PBS, PBS + L, Py-Cage, and Py-Cage + L were set and Py-Cage (40 μg/mL) were added into fresh cell medium in the Py-Cage, and Py-Cage + L groups and incubated with cells for 6 h. PBS and PBS + L groups were irradiated with white light (80 mW·cm^{-2}) for 10 min (48 J·cm^{-2}), and then cells were rinsed with PBS and trypsin zed by trypsin for collecting the cell suspensions. Cells after centrifugation of the suspension were incubated with the mixture of Annexin V-FITC and PI in dark for 10 min. After rinsed with PBS, all samples were measured with FACS Calibur flow cytometer using 488 nm laser for Annexin V-FITC and 561 nm laser for PI excitation.

Construction of tumor models.

Five weeks old female BALB/c mice were provided by the Animal Center of Southern Medical University. All animal experiments were carried out under the guidance of the protocols approved by the local Ethical Committee in compliance with the Chinese law on experimental animals and followed regulations of the Institutional Animal Care and Use Committee of South Medical University. All mice were kept in SPF-level feeding conditions with adequate water and food. The temperature is kept at 26 °C, the humidity is 50 % and a 12 h light/dark cycle. Female mice (BALB/c, 6-8 weeks old) were inoculated subcutaneously with mouse breast cancer cells. 100 μL 4T1 cells (2 × 10^6) suspensions

were injected subcutaneously into the right limb of the mice to obtain a Breast cancer model. When tumors reached an average volume of 80 mm^3, mice were used for in vivo imaging and PDT evaluation (Volume=length*width*width /2).

***In vivo* PDT assay.**

When the volume of tumors grew to about 80 mm^3, Py-Cage (300 μg/mL, 100 μL) was injected intratumorally into the tumors, The distribution of Py-Cage in mice was observed by the IVIS Lumina II (E_m = cy5.5, E_x = 430 nm, exposure time = 5 s) after the injection of 0.5, 2, 4, 8, 12 and 24 hours. 2 h was chosen as the administration time based on the distribution of Py-Cage injection into the tumor. The tumor-bearing mice were randomly divided into four groups, including: PBS, PBS + L, Py-Cage, and Py-Cage + L groups. 100 μL PBS was injected intratumorally into the tumors of each mouse in PBS and PBS + L groups. And 100 μL Py-Cage (300 μg/mL) was injected intratumorally into the tumors of each mouse in Py-Cage and Py-Cage + L groups. After 2 h, the mice in PBS + L, and Py-Cage + L groups were irradiated with white light of 80 $mW \cdot cm^{-2}$ for 10 min (48 $J \cdot cm^{-2}$), while PBS and Py-Cage groups were not irradiated. Tumor size and weight of mice were recorded every other day after treatment. After 14 days of treatment, the mice were sacrificed, and the heart, liver, spleen, lung and kidney organs were removed and fixed with 4% paraformaldehyde for H&E staining to determine whether Py-Cage caused organ damage. In addition, Py-Cage (300 μg/mL, 100 μL) was injected into the healthy mice without tumor through tail vein, and PBS group was used as the control group. 24 hours after injection, blood samples were collected from mice for detection of hematological markers. Through the detection and analysis of blood parameters such as red blood cells, white blood cells and platelets, to determine whether there are infection, anemia, bleeding and other abnormalities in mice after injection of Py-Cage through tail vein to prove the biological safety of Py-Cage.

Biocompatibility and biosafety on rats.

Healthy rats were further used to study the biocompatibility of Py-Cage, and Py-Cage, where Py-Cage was intravenously injected into healthy rats through the tail vein (300 μg/mL, 100 μL/rat). After 48 h, the rats were euthanized, blood was taken out from the tail of anesthetized rats and the organs were extracted. Finally, H&E staining was performed on the organs, and the blood routine and biochemical indicators of the rats were tested, as well as the levels of cytokines (CK) in the rats serum.

Synthesis of Py-Cage NPs.

A DMSO solution of DSPE-PEG_{2000} (0.2 mL, 10 mg/mL) was evenly mixed with Py-Cage solution (0.2 mL, 5 mg/mL) in DMSO. The above mixed solution was added to 9 mL of ultrapure water under ultrasonic sonication with a power of 100 W, which was further sonicated for 2 min. The obtained mixture was dialyzed with a dialysis membrane (with molecular cutoff of 30 kDa) for 2 days, and the ultrapure water was replaced several times. The aqueous solution of Py-Cage NPs was finally obtained after passing through a 450 μm filter membrane.

***In vivo* PDT assay of Py-Cage NPs.**

4T1 tumor bearing mouse model was established by subcutaneously inoculating 4T1 breast cancer cells (2×10^6) into the right hind leg of nude mice (BALB/c-nude, 6-8 weeks old). When the tumor volume reaches approximately 80 mm^3, the mice were randomly divided into four groups including PBS, PBS+L, Py-Cage NPs, and Py-Cage NPs+L groups (n = 4 mice per group). Py-Cage NPs (300 μg/mL, 100 μL/mouse) was injected into the selected mice through the tail vein. The distribution of Py-Cage NPs in mice was observed by the IVIS Lumina II (AniView Phoenix) (E_m = 680 nm, E_x = 430 nm, exposure time = 1 s) after 0, 2, 4, 6, and 8 h post injection. At 6 h post injection, the selected mice were exposed to light irradiation at a power of 80 $mW \cdot cm^{-2}$ for 10 min (48 $J \cdot cm^{-2}$). These mice were received a second injection of Py-Cage NPs and light exposure on the third day post injection. The weight of the mice and the volume of the tumor were recorded every two days. At day 10 post

injection, the mice were euthanized, and the tumors were extracted. Finally, H&E staining was performed on the organs and tumors of the mice.

Statistical Analysis.

Data between two groups were analyzed by an independent *t* test, and more than two groups were tested by one-way ANOVA followed by a suitable post-hoc analysis. For all tests, $P < 0.05$ was considered statistically significant. Data were expressed as the mean ± SD (standard deviation). All data were analyzed using GraphPad Prism 8.0 software.

Reference

1. Hu, H.; Wang, H.; Yang, Y.; Xu, J.; Zhang, X. A Bacteria-Responsive Porphyrin for Adaptable Photodynamic/Photothermal Therapy. *Angew. Chem. Int. Ed.* **2022**, *61*, e202200799.
2. Sadegh, F.; Bagheri, O.; Moghadam, M.; Mirkhani, V.; Tangestaninejad, S.; Mohammadpoor-Baltork, I. Palladium(II) Tetrakis(4-*N*,*N*,*N*-Trimethylammoniumphenylene)Porphyrin Supported on Ion-Exchange Resins as Efficient and Reusable Catalysts for C–C Coupling Reactions. *J. Organomet. Chem.* **2014**, *759*, 46–57.
3. Li, X.; Qiu, J.; Zhang, L.; Mu, J. *In-situ* Synthesis and Photoluminescence of a Europium Porphyrin Complex Incorporated in the Silica Matrix. *J. Dispers. Sci. Technol.* **2007**, *28* (7), 1081–1085.
4. Chen, L.; Bai, H.; Xu, J.-F.; Wang, S.; Zhang, X. Supramolecular Porphyrin Photosensitizers: Controllable Disguise and Photoinduced Activation of Antibacterial Behavior. *ACS Appl. Mater. Interfaces* **2017**, *9* (16), 13950–13957.
5. Zhu, Z.-H.; Liu, Y.; Song, C.; Hu, Y.; Feng, G.; Tang, B. Z. Porphyrin-Based Two-Dimensional Layered Metal–Organic Framework with Sono-/Photocatalytic Activity for Water Decontamination. *ACS Nano* **2022**, *16* (1), 1346–1357.
6. Gan, S.; Wu, W.; Feng, G.; Wang, Z.; Liu, B.; Tang, B. Z. Size Optimization of Organic Nanoparticles with Aggregation-Induced Emission Characteristics for Improved ROS Generation and Photodynamic Cancer Cell Ablation. *Small* **2022**, *18* (26), 2202242.
7. Yu, Y.; Wu, S.; Zhang, L.; Xu, S.; Dai, C.; Gan, S.; Xie, G.; Feng, G.; Tang, B. Z. Cationization to Boost Both Type I and Type II ROS Generation for Photodynamic Therapy. *Biomaterials* **2022**, *280*, 121255.

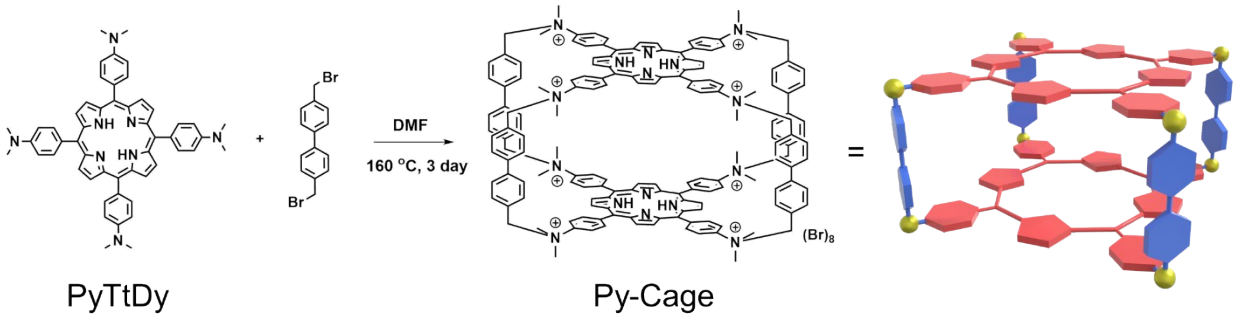

Scheme S1. Synthetic route of Py-Cage and the schematic diagram of Py-Cage.

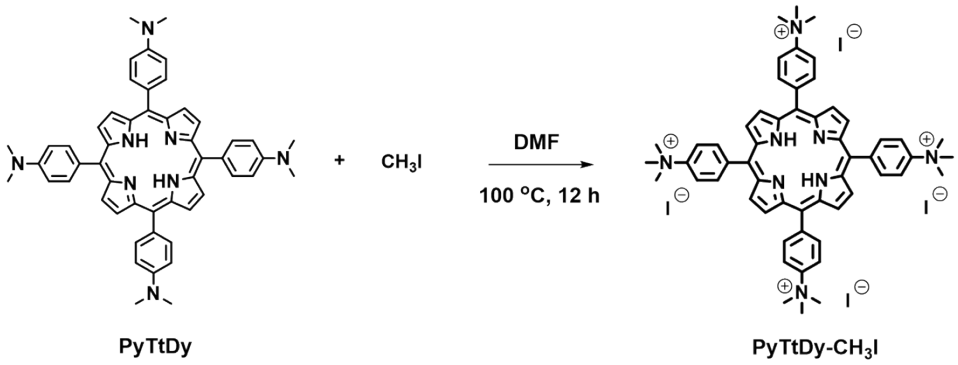

Scheme S2. Synthetic route of PyTtDy-CH_3I.

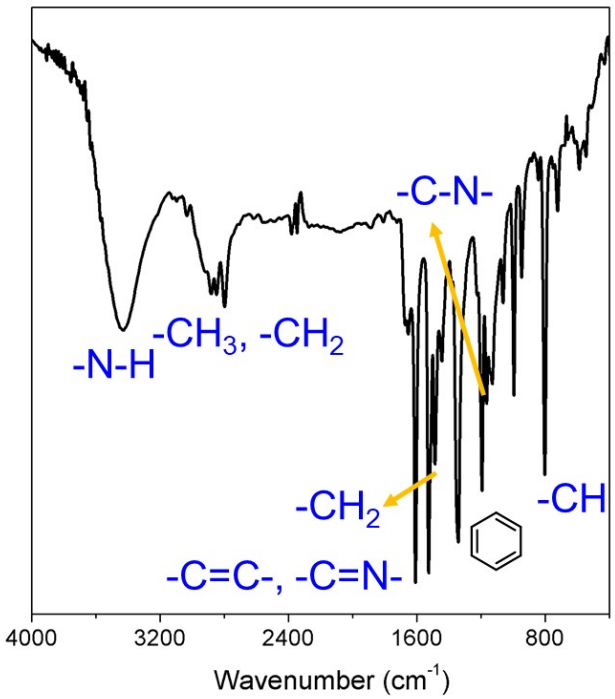

Figure S1. Fourier transform infrared spectroscopy (FTIR) of Py-Cage. Fourier transform infrared spectroscopy (FTIR) results show that 3430 cm^{-1} is the stretching vibration of the -N-H bond on the pyrrole ring; 2882 cm^{-1}, 2847 cm^{-1}, and 2795 cm^{-1} are the stretching vibrations of $-CH_3$ and $-CH_2$ and

antisymmetric stretching vibration; 1606 cm^{-1} and 1525 cm^{-1} are the stretching vibrations of -C=C- on the benzene ring and -C=N- bonds on the pyrrole ring; 1488 cm^{-1} is the stretching vibration of -CH_2; 1342 cm^{-1} and 1193 cm^{-1} is the stretching vibration of the -C-H bond on the benzene ring; 1165 cm^{-1} is the stretching vibration of the -C-N- bond; 802 cm^{-1} is the bending vibration of the symmetry plane of the -C-H bond on the benzene ring.

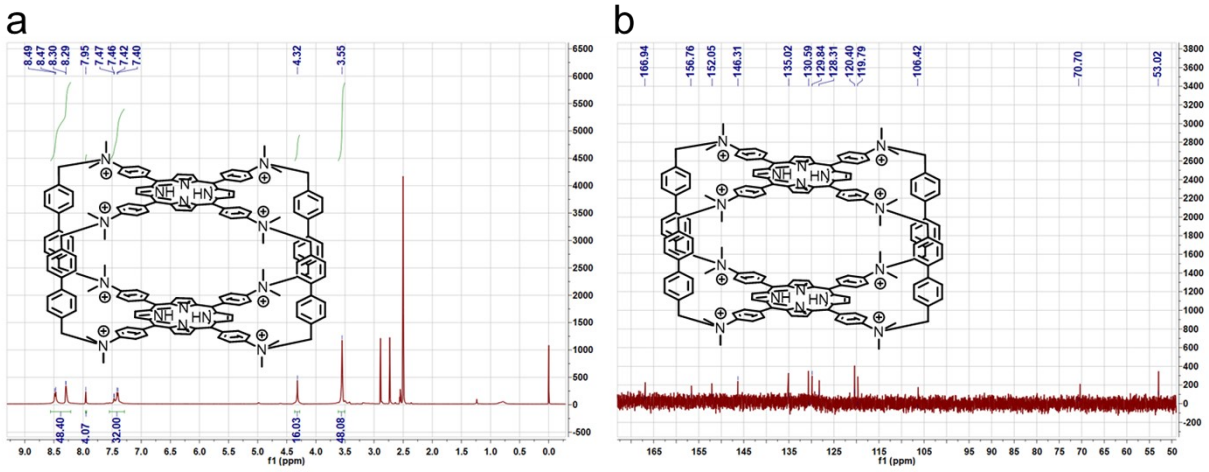

Figure S2. The ^{1}H (a) and ^{13}C (b) NMR spectra of Py-Cage in DMSO-d_6.

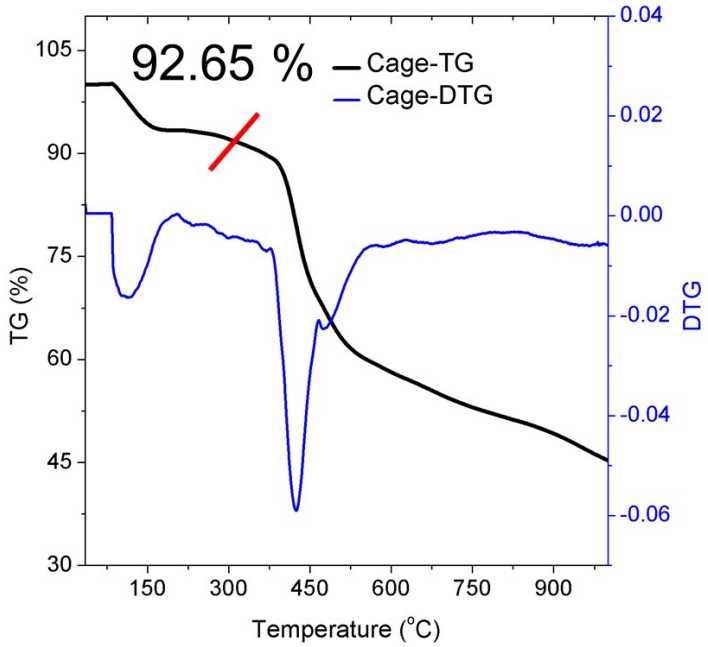

Figure S3. TG and DTG curves of Py-Cage.

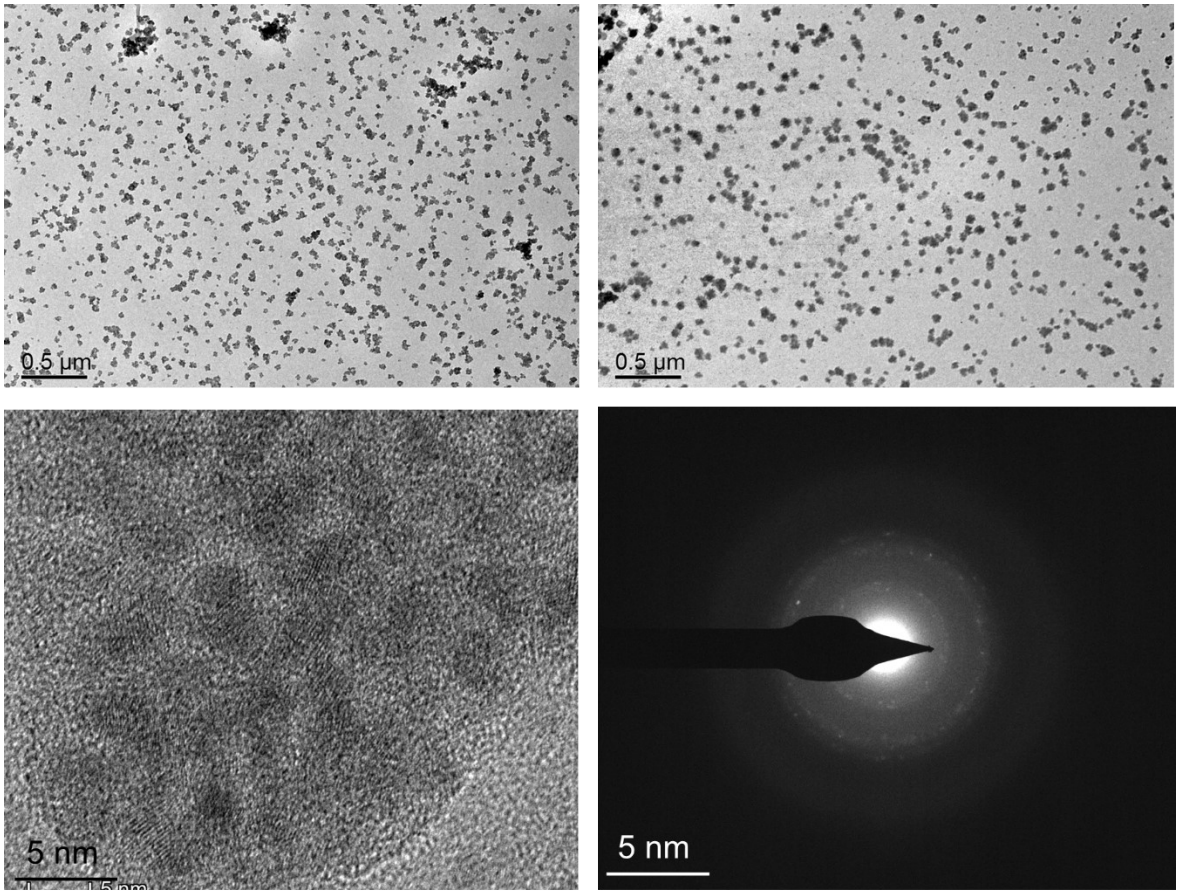

Figure S4. TEM and HRTEM images of Py-Cage after dissolving in mixture solvent H_2O/DMSO (V_{water}/V_{DMSO} = 99:1).

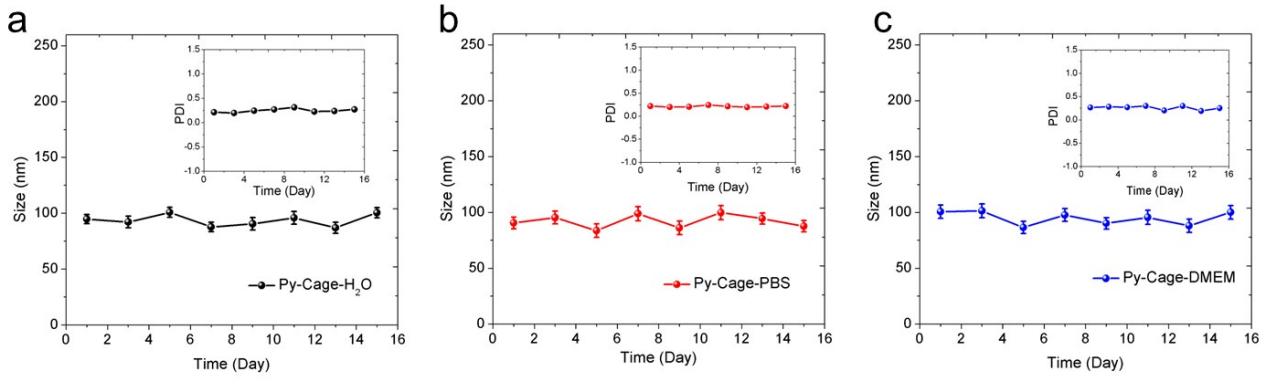

Figure S5. The tracking results of the size and PDI changes of Py-Cage in H_2O (a), PBS (b) and dulbecco's modified eagle medium (DMEM, c) conditions respectively within 15 days. Data presented mean ± SD, n = 3.

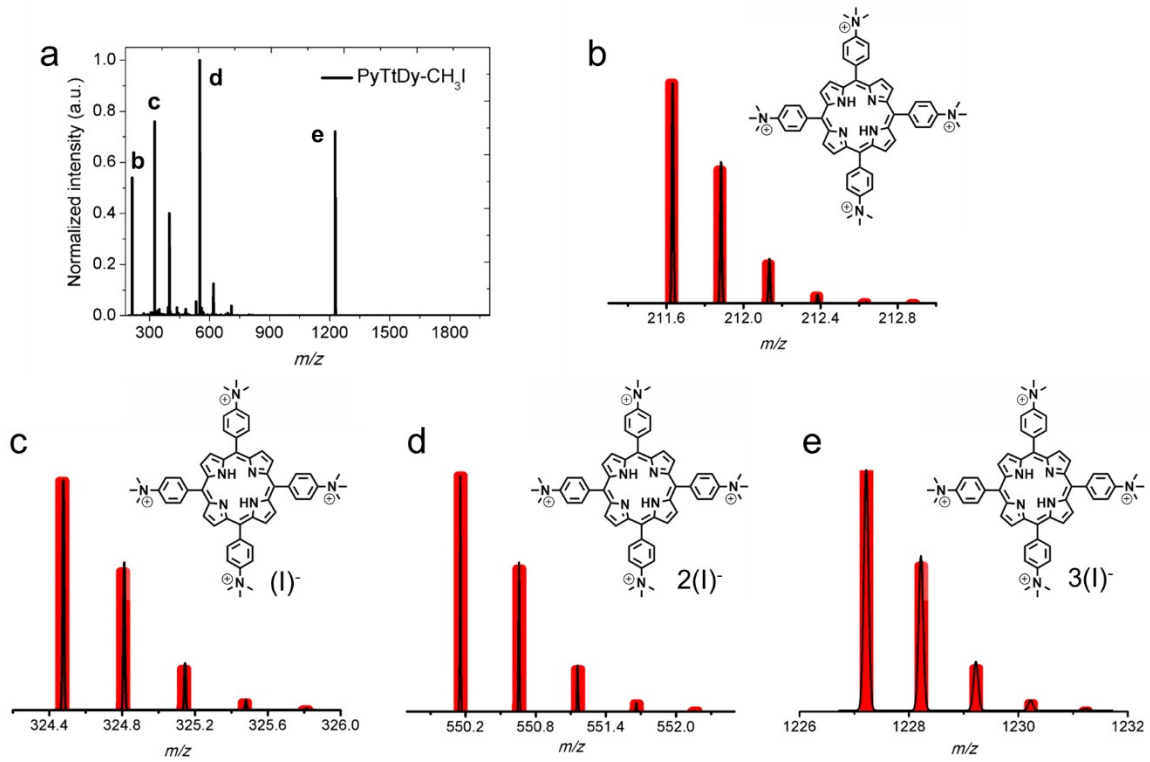

Figure S6. (a) High-resolution electrospray mass spectrometry (HRESI-MS) of PyTtDy-CH_3I, (b-e) black is the experimental value, red is the theoretical value.

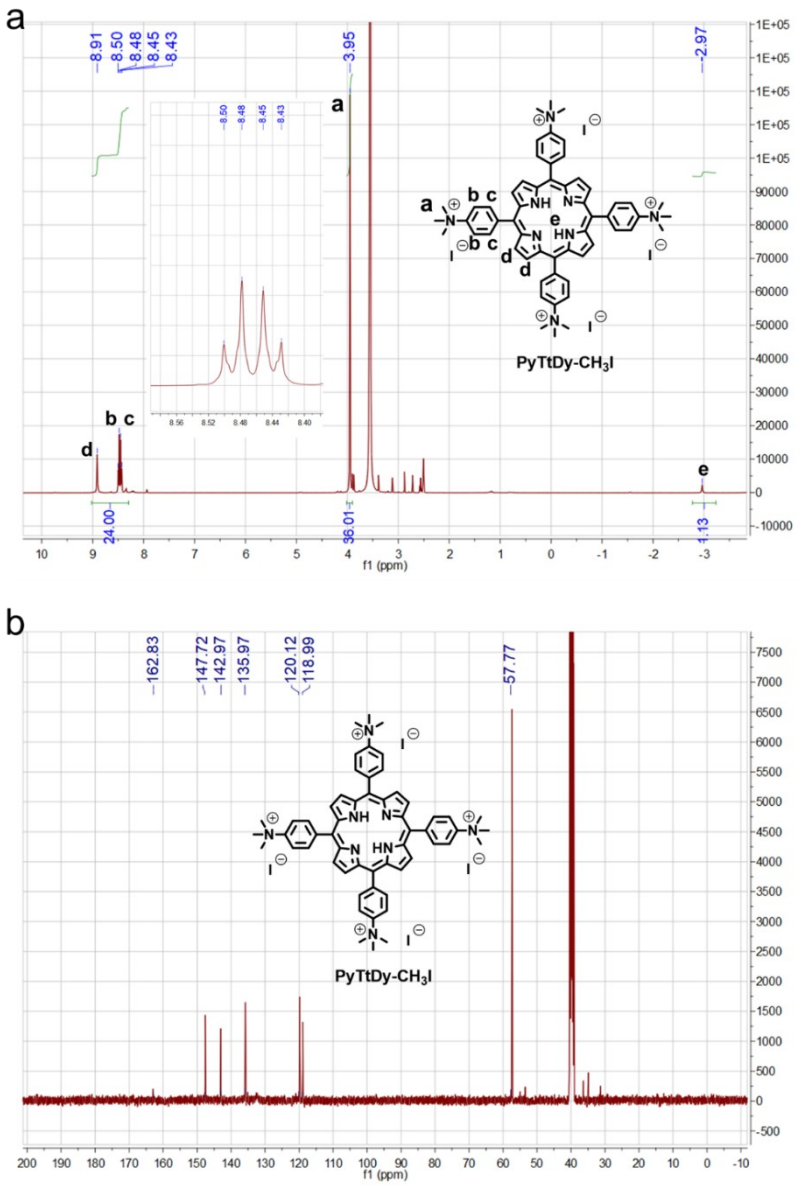

Figure S7. The ^{1}H (a) and ^{13}C (b) NMR spectra of PyTtDy-CH_3I in DMSO-d_6.

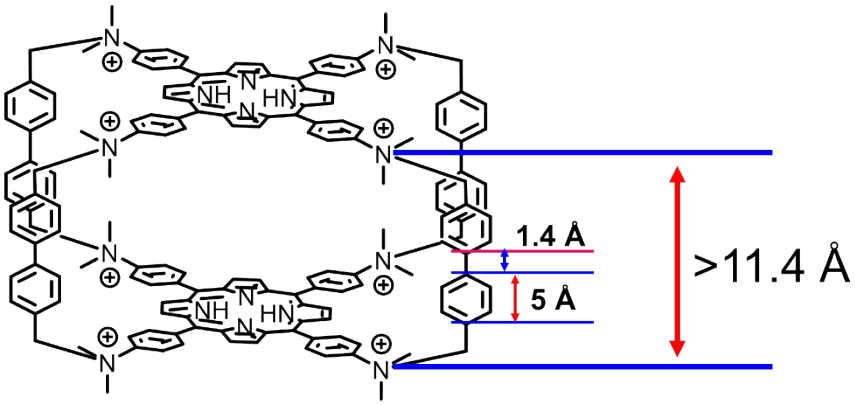

Figure S8. Schematic of Py-Cage to show the distance between the upper and lower layers of PyTtDy in Py-Cage, the length of a benzene ring is about 5 Å, and the -C-C- bond length is 1.4 Å, therefore, the distance between the upper and lower layers of PyTtDy is greater than 11.4 Å.

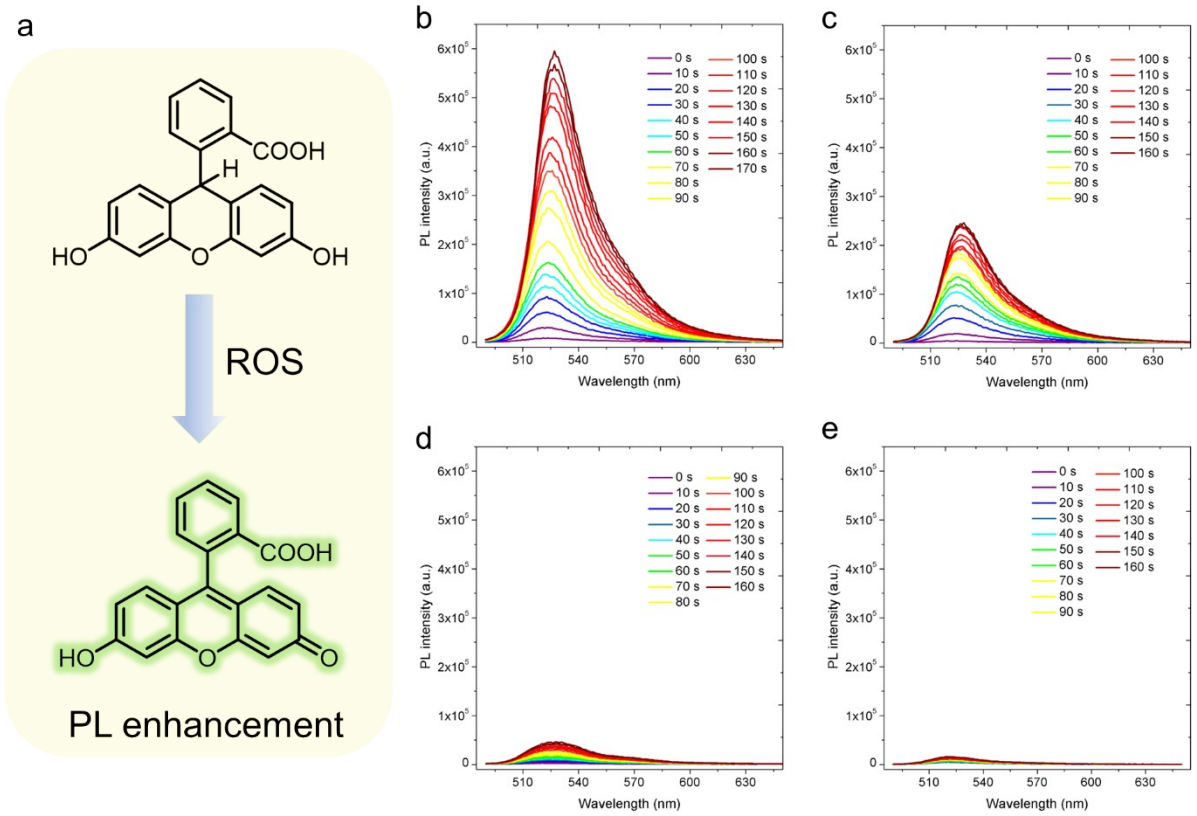

Figure S9. (a) ROS detection mechanism of DCFH; The PL spectrum changes of DCFH (50 μM) in the presence of Py-Cage (b), PyTtDy-CH_3I (c) and PyTtDy (d) (10 μg/mL) upon light irradiation (20 $mW \cdot cm^{-2}$) in mixture solvent H_2O/DMSO (V_{water}/V_{DMSO} = 99:1); (e) The PL spectra of DCFH (50 μM) under the irradiation with different time (20 $mW \cdot cm^{-2}$) in mixture solvent H_2O/DMSO (V_{water}/V_{DMSO} = 99:1).

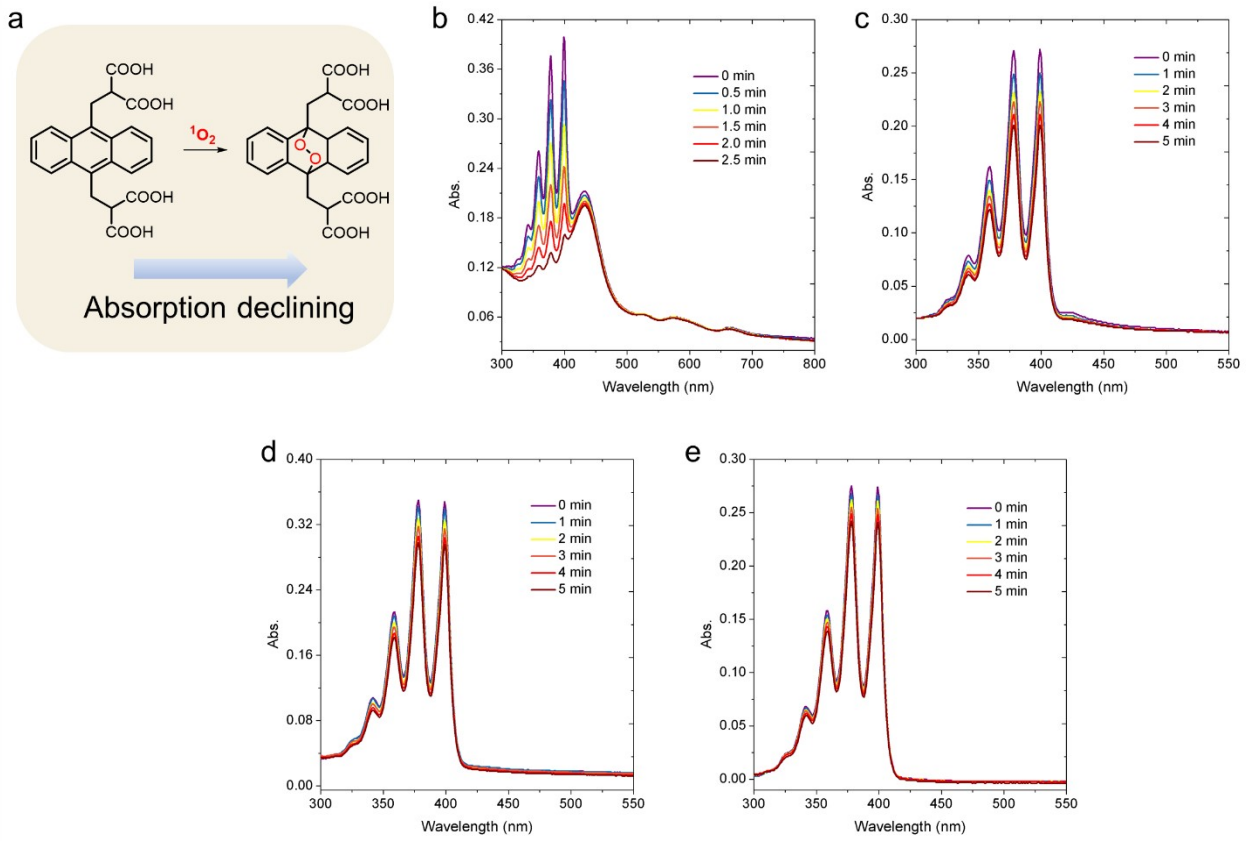

Figure S10. (a) $^1O_2$ detection mechanism of ABDA; Absorption spectrum changes of ABDA (20 μM) in the presence of Py-Cage (b), PyTtDy-CH_3I (c) and PyTtDy (d) in mixture solvent H_2O/DMSO (V_{water}/V_{DMSO} = 99:1) under the irradiation (20 mW·cm^{-2}) with different duration; (e) The UV-vis absorption spectra of ABDA (20 μM) under the irradiation with different time (20 mW·cm^{-2}) in mixture solvent H_2O/DMSO (V_{water}/V_{DMSO} = 99:1).

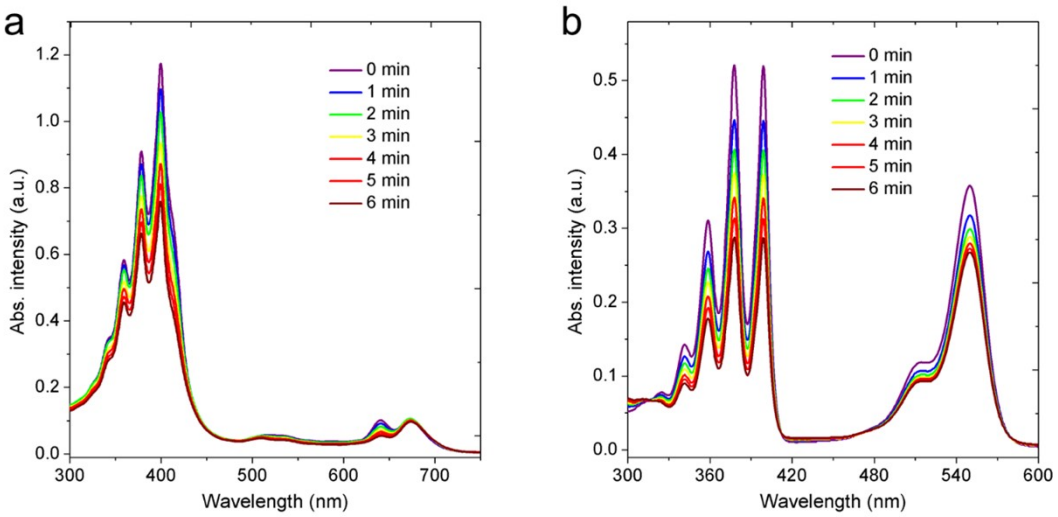

Figure S11. Absorption spectrum changes of ABDA (20 μM) in the presence of Ce6 (a) and RB (b) (10 μg/mL) in mixture solvent H_2O/DMSO (V_{water}/V_{DMSO} = 99:1) under the irradiation (20 mW·cm^{-2}) with different duration.

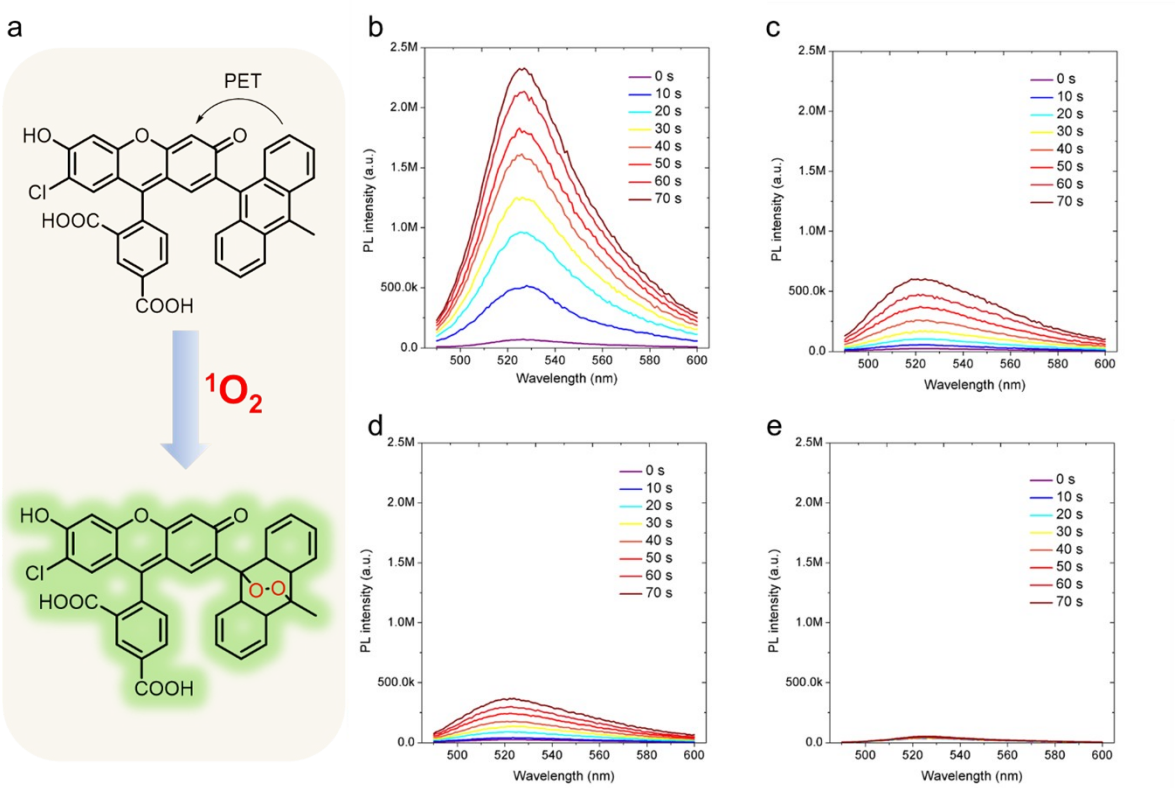

Figure S12. (a) $^1O_2$ detection mechanism of SOSG; the PL spectrum changes of SOSG (20 μM) in the presence of Py-Cage (b), PyTtDy-CH_3I (c) and PyTtDy (d) (10 μg/mL) upon light irradiation (20 mW·cm^{-2}) in mixture solvent H_2O/DMSO (V_{water}/V_{DMSO} = 99:1); (e) The PL spectra of SOSG (20 μM) under the irradiation with different time (20 mW·cm^{-2}) in mixture solvent H_2O/DMSO (V_{water}/V_{DMSO} = 99:1).

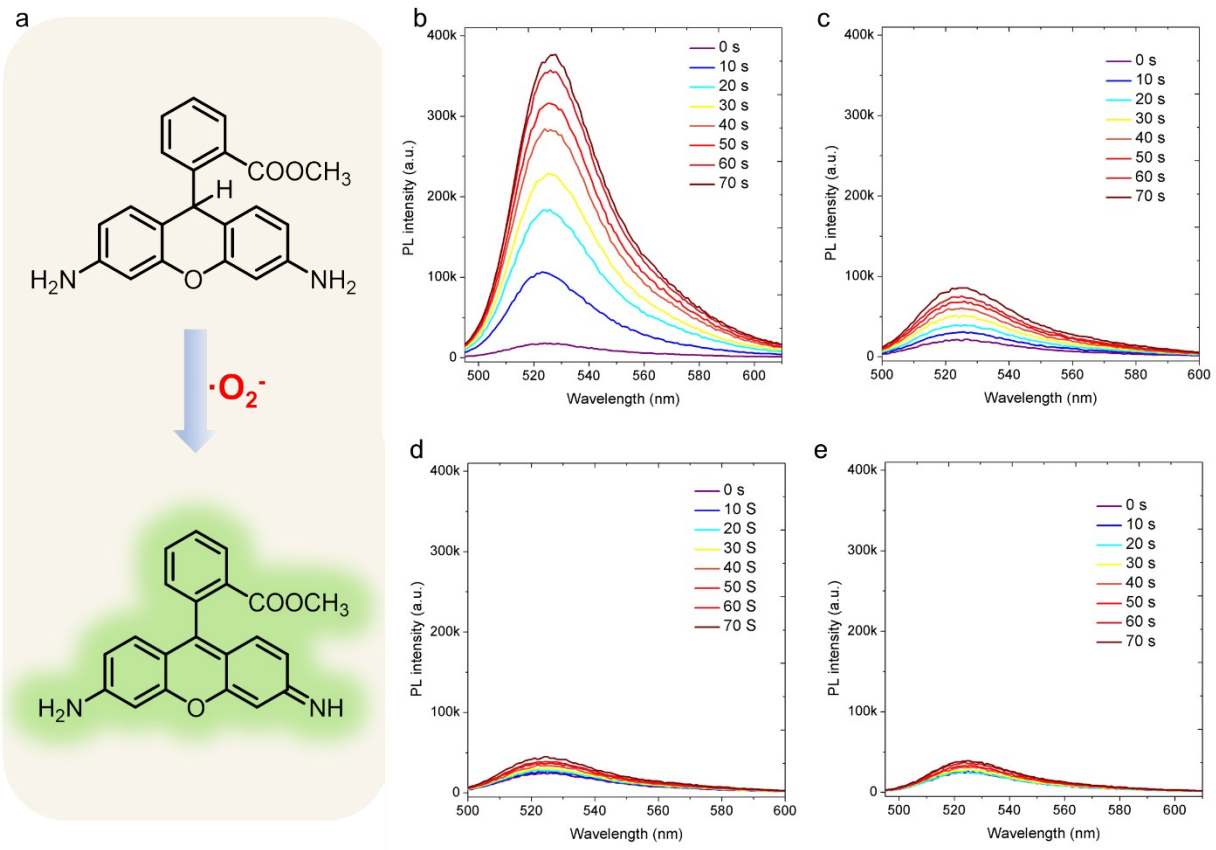

Figure S13. (a) $\cdot O_2^-$ detection mechanism of DHR123; The PL spectrum changes of DHR123 (20 μM) in the presence of Py-Cage (b), PyTtDy-CH_3I (c) and PyTtDy (d) (10 μg/mL) upon light irradiation (20 mW·cm^{-2}) in mixture solvent H_2O/DMSO (V_{water}/V_{DMSO} = 99:1); (e) The PL spectra of DHR123 (20 μM) under the irradiation with different time (20 mW·cm^{-2}) in mixture solvent H_2O/DMSO (V_{water}/V_{DMSO} = 99:1).

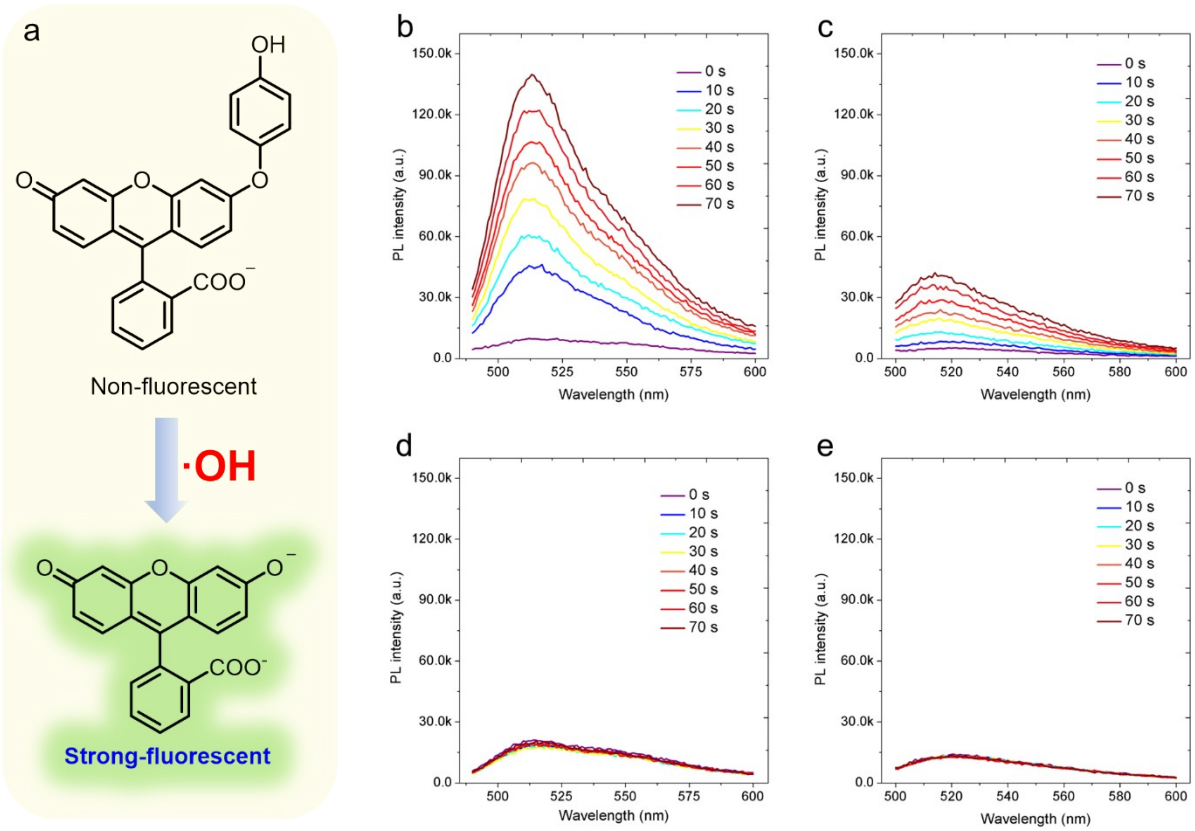

Figure S14. (a) ·OH detection mechanism of HPF; The PL spectrum changes of HPF (20 μM) in the presence of Py-Cage (b), PyTtDy-CH_3I (c) and PyTtDy (d) (10 μg/mL) upon light irradiation (20 mW·cm^{-2}) in mixture solvent H_2O/DMSO (V_{water}/V_{DMSO} = 99:1); (e) The PL spectra of HPF (20 μM) under the irradiation with different time (20 mW·cm^{-2}) in mixture solvent H_2O/DMSO (V_{water}/V_{DMSO} = 99:1).

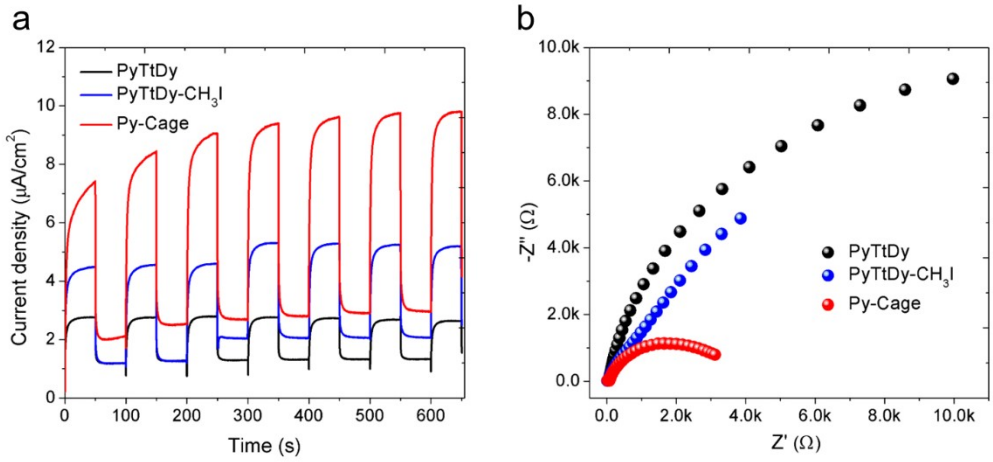

Figure S15. Comparison of photocurrent signals and electrochemical impedance spectroscopy (EIS) of PyTtDy, PyTtDy-CH_3I and Py-Cage.

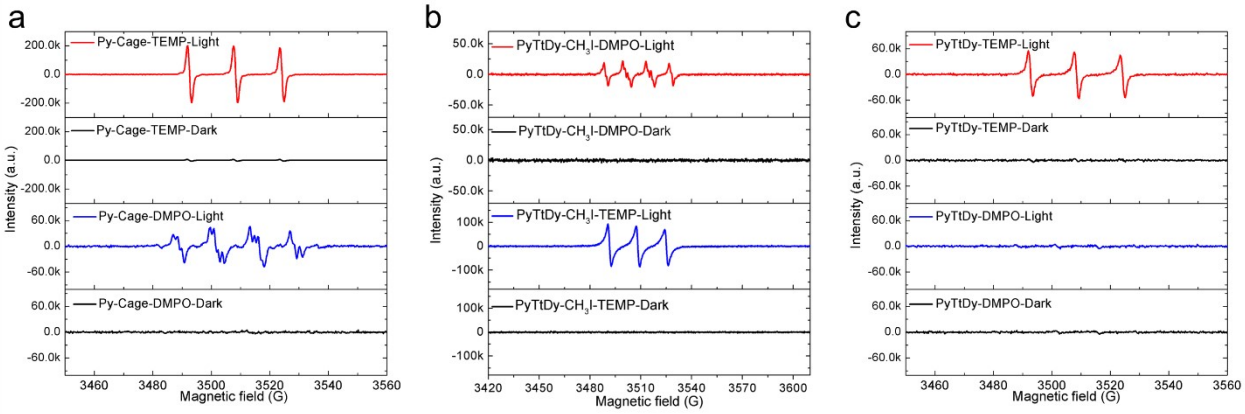

Figure S16. Electron paramagnetic resonance (EPR) spectra of DMPO−·O_2^-, DMPO−·OH and TEMP−$^1O_2$ for Py-Cage (a), PyTtDy-CH_3I (b) and PyTtDy (c) before and after light irradiation.

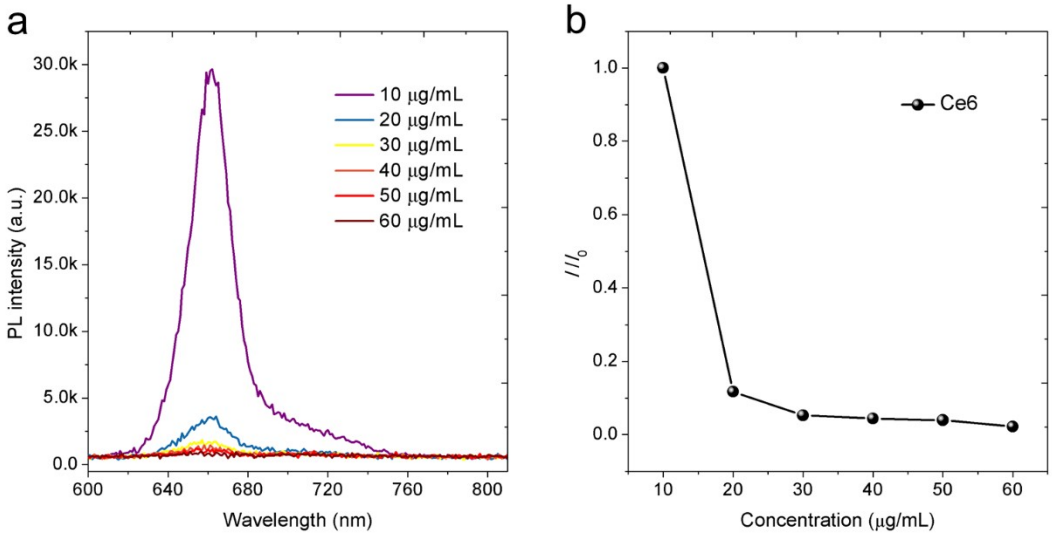

Figure S17. Fluorescence (PL) spectra (a) and intensity changes at 662 nm (b) of Ce6 aqueous solutions with different concentrations.

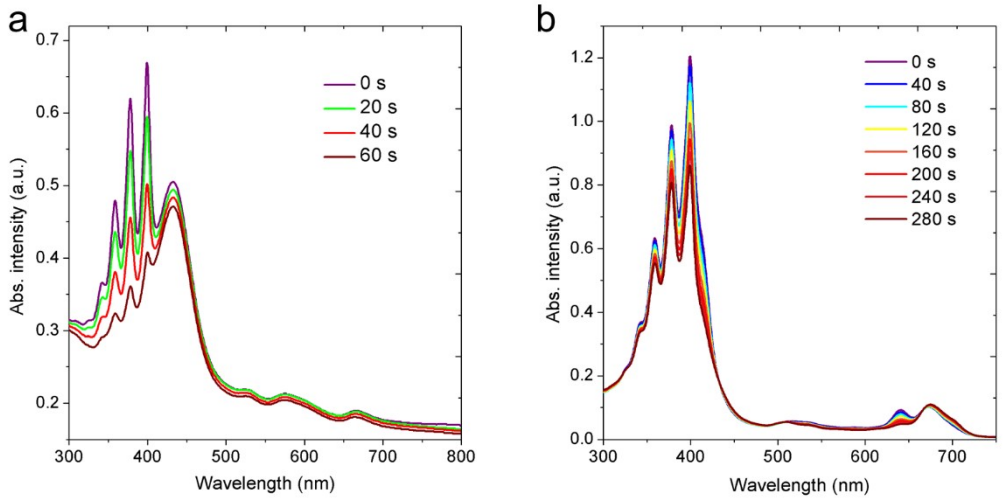

Figure S18. Absorption spectrum changes of ABDA (20 μM) in the presence of Py-Cage (a) and Ce6 (b) in mixture solvent H_2O/DMSO (V_{water}/V_{DMSO} = 99:1) under the irradiation (20 mW·cm^{-2}) with different duration in an oxygen environment.

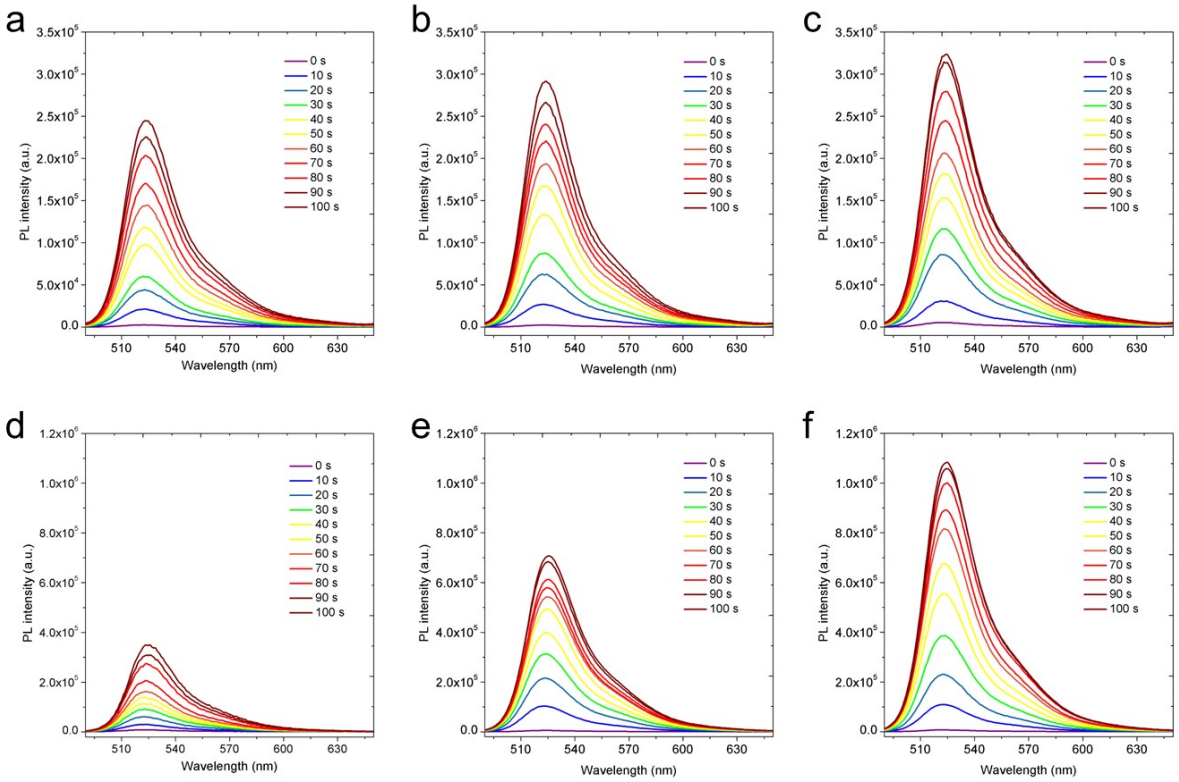

Figure S19. Fluorescence spectrum changes of DCFH (50 μM) containing different concentrations of Ce6 (a-c, 10 μg/mL-20 μg/mL) and Py-Cage (d-f, 10 μg/mL-20 μg/mL), respectively, and under light irradiation conditions (20 mW·cm^{-2}).

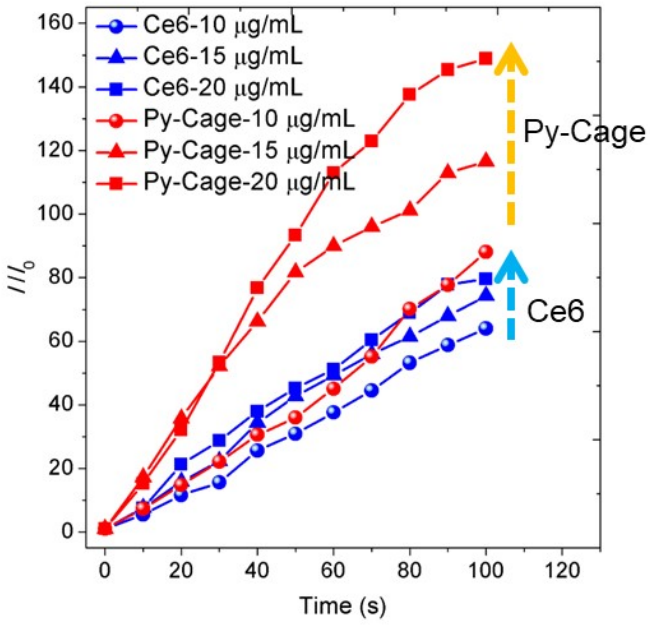

Figure S20. Comparison of fluorescence changes (I / I_0) of DCFH with different concentrations of Ce6 and Py-Cage under light irradiation.

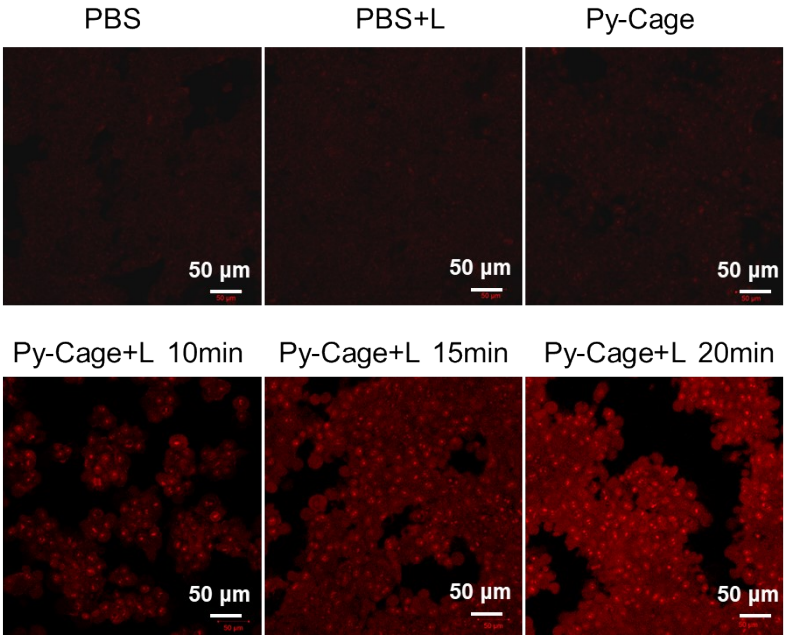

Figure S21. The dihydroethidium (DHE) probe was used to detect the production of $\cdot O_2^-$ after co-incubation of Py-Cage (40 μg/mL) with 4T1 cancer cells and under white light irradiation (60 mW·cm^{-2}), and the red fluorescence was the fluorescein produced by DHE in response to $\cdot O_2^-$.

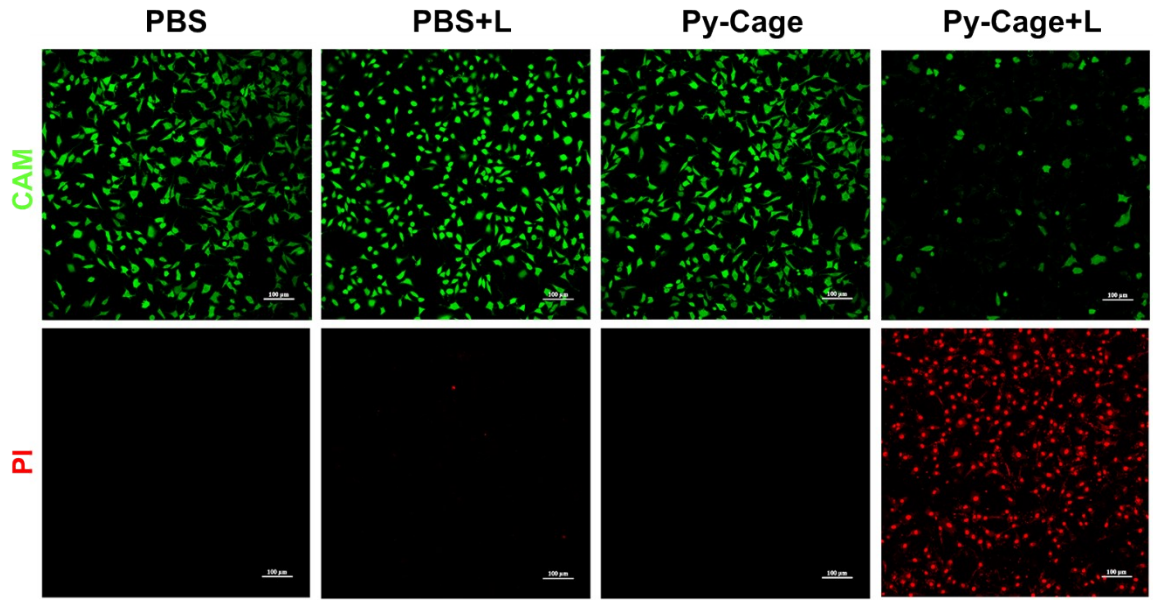

Figure S22. Live/dead cell staining of 4T1 cells co-incubated assays after different treatment, live cells were stained green by CAM and dead cells were stained red by PI. Scale bar = 100 μm.

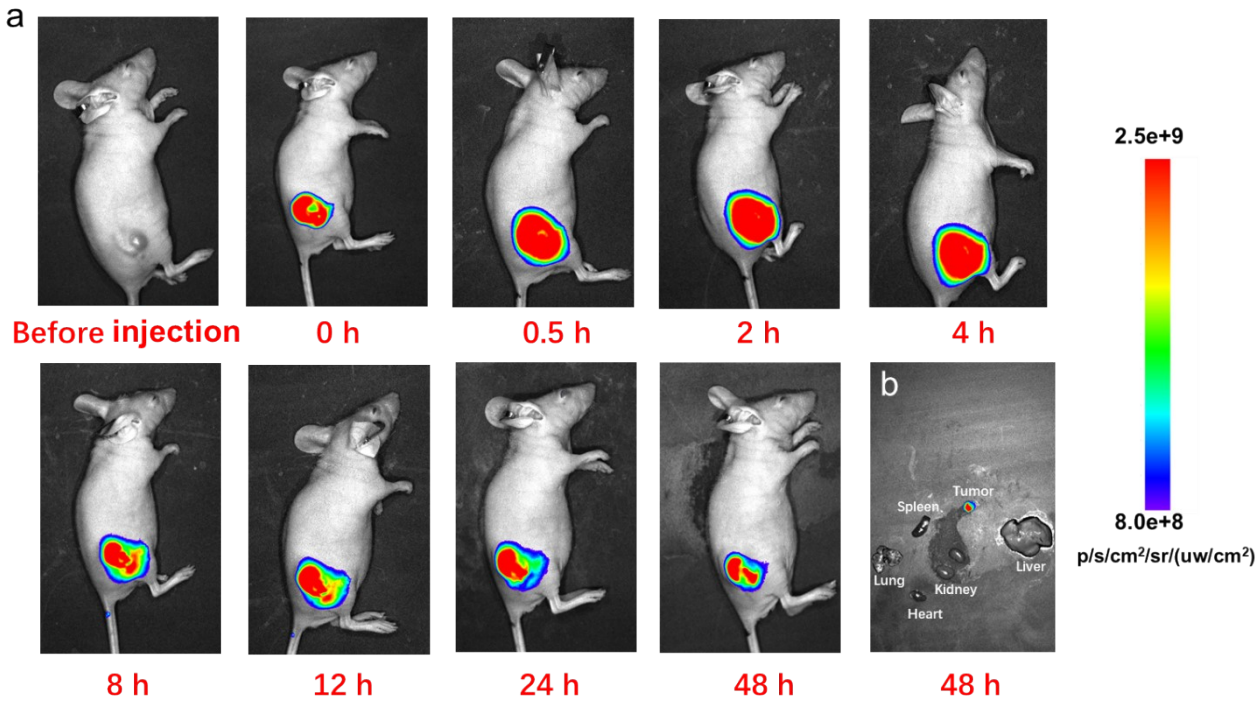

Figure S23. (a) Fluorescence images of tumor bearing mice at different times after Py-Cage injection (300 μg/mL, 100 μL); (b) Py-Cage distribution in mouse major organs and tumors collected at 48 h post injection.

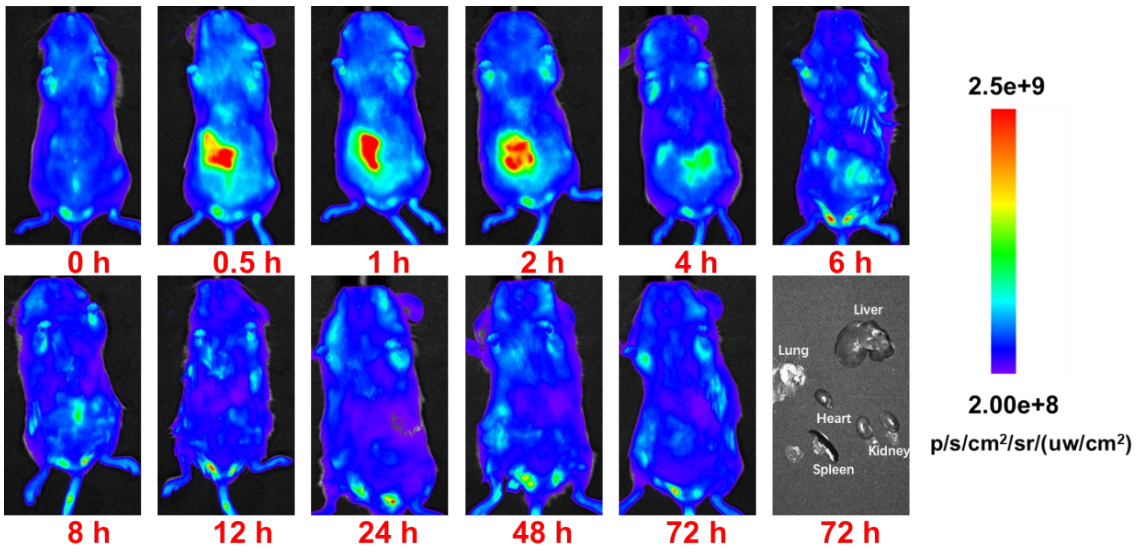

Figure S24. Fluorescence images of healthy mice at different times after Py-Cage injection through tail vein, and the ex vivo fluorescence imaging of various vital organs of mice at 72 h post injection.

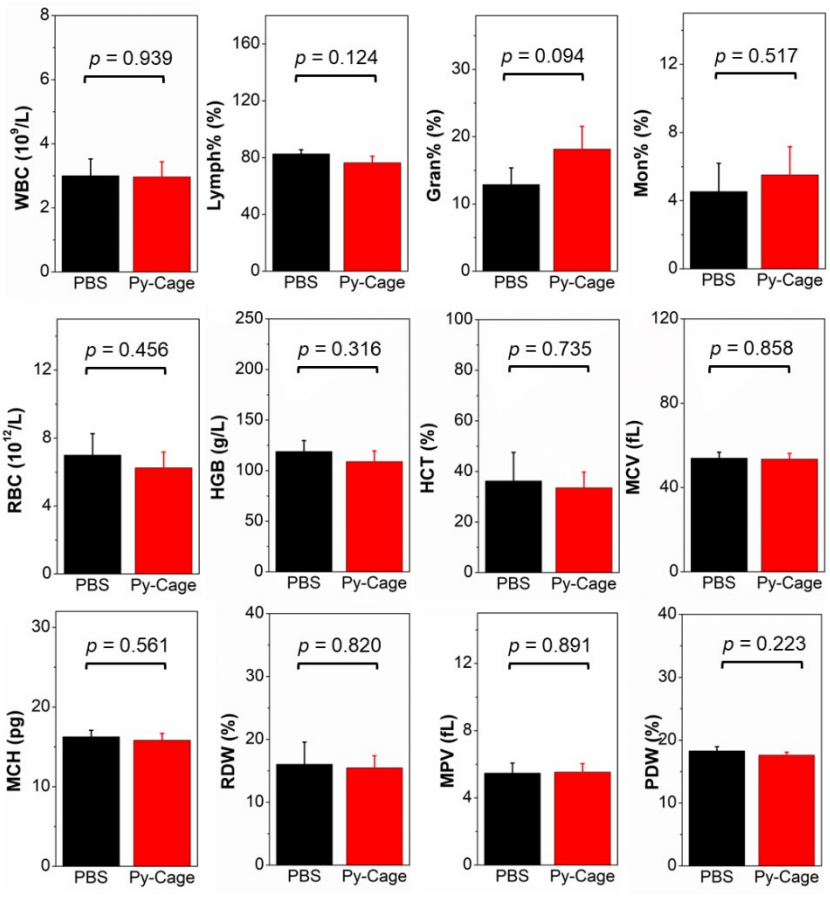

Figure S25. Blood routine parameters (white blood cells (WBC and MON), lymphocytes (LYMPH), neutrophils (GRAN), red blood cells (RBC), hematocrit (HCT), hemoglobin (HGB), mean muscle tone

(MCV), erythrocyte hemoglobin content (MCH), erythrocyte distribution width (RDW), platelet volume (MPV) and platelet volume distribution width (PDW)) of normal mice injected with PBS or Py-Cage, respectively. Data presented mean ± SD, n = 3, No significant difference.

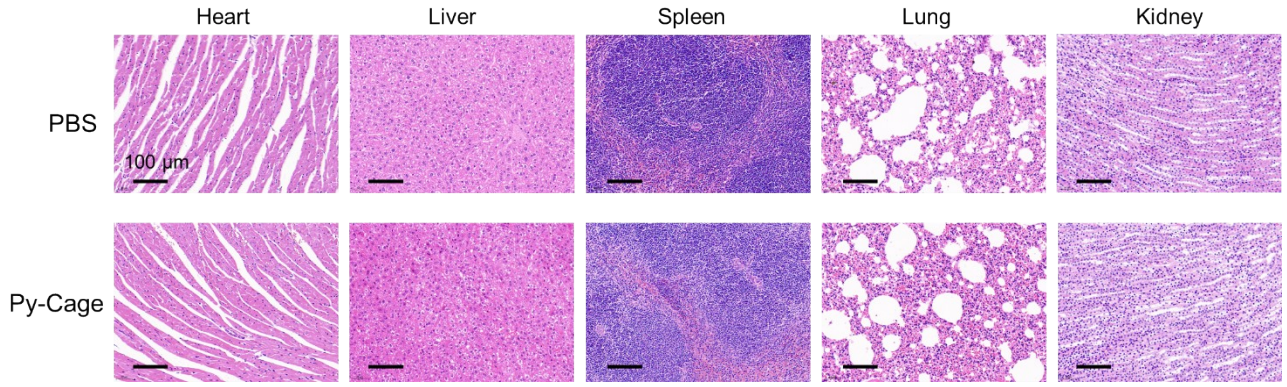

Figure S26. H&E staining images of major organ sections of normal mice treated with PBS or Py-Cage. Scale bar = 100 μm.

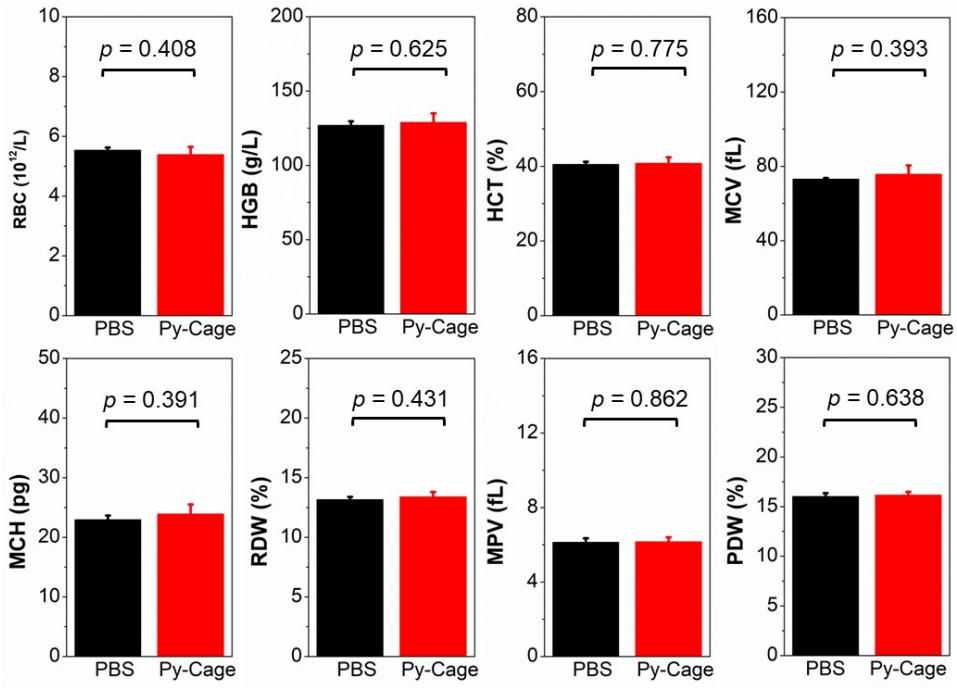

Figure S27. Some important blood routine parameters (red blood cells (RBC), hematocrit (HCT), mean muscle tone (MCV), erythrocyte hemoglobin content (MCH), erythrocyte distribution width (RDW), hemoglobin (HGB), Platelet volume (MPV) and platelet volume distribution width (PDW)) of healthy rats injected with PBS or Py-Cage, respectively. Data presented mean ± SD, n = 3, No significant difference.

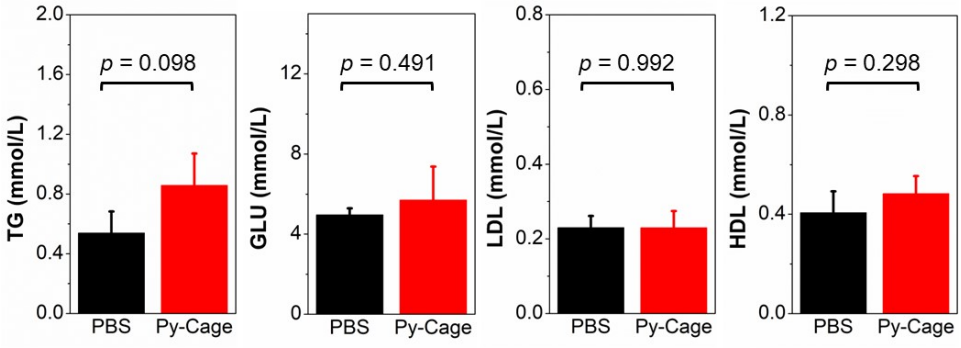

Figure S28. Some important blood biochemical parameters (low-density lipoprotein (LDL), triglyceride (TG), high-density lipoprotein cholesterol (HDL), glucose (GLU)) of healthy rats injected with PBS or Py-Cage, respectively. Data presented mean ± SD, n = 3, No significant difference.

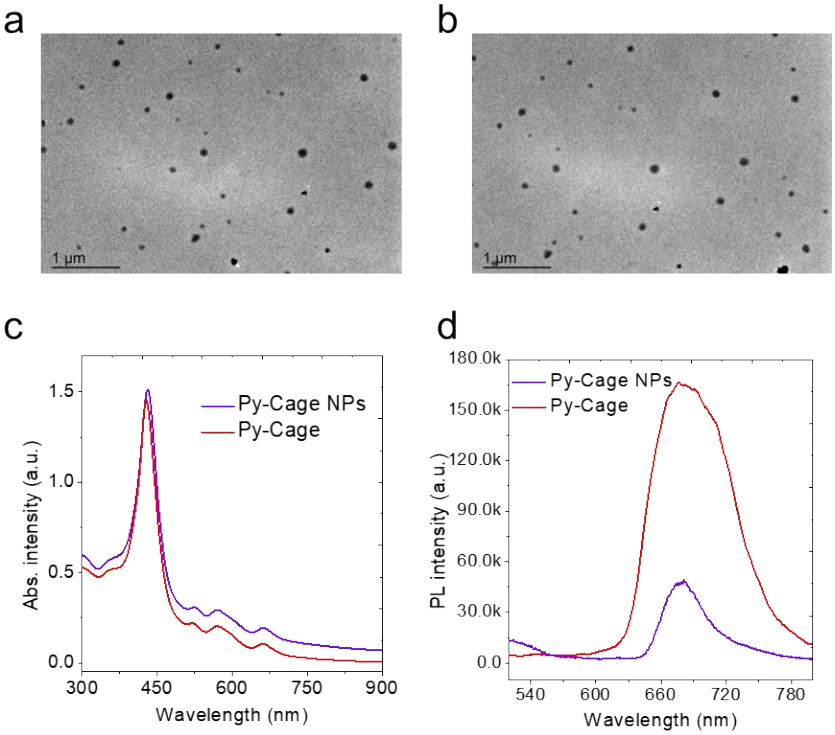

Figure S29. (a and b) TEM images of Py-Cage NPs. Comparison of UV-Vis absorption spectra (c) and fluorescence spectra (d) of Py-Cage and Py-Cage NPs under the same concentration conditions (10 μg/mL).

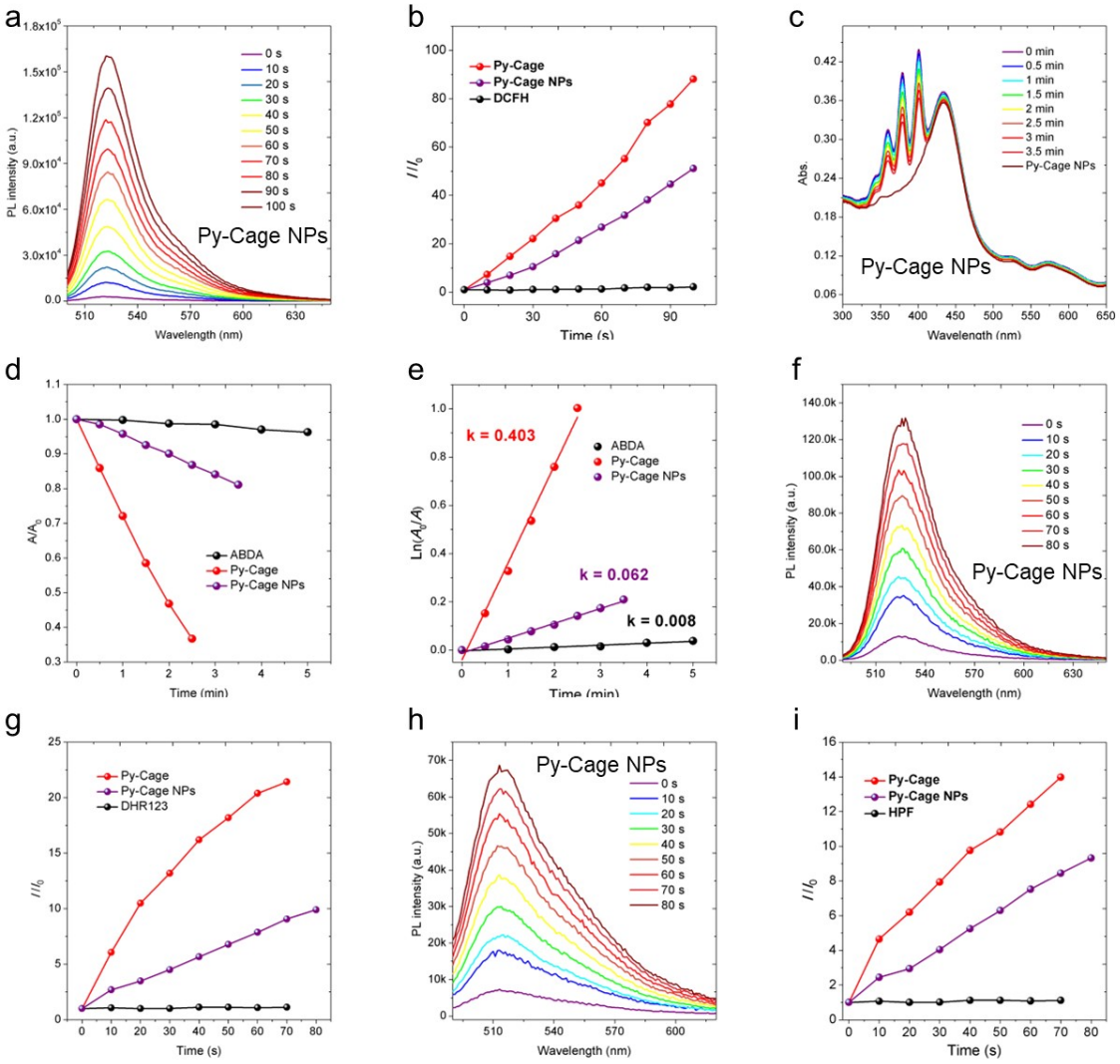

Figure S30. (a) The PL spectrum changes of DCFH (50 μM) in the presence of Py-Cage NPs (10 μg/mL) upon light irradiation (20 mW·cm^{-2}) in H_2O; (b) the ROS production of Py-Cage, Py-Cage NPs (10 μg/mL) under white light irradiation (white light, 20 mW·cm^{-2}) using DCFH as an indicator; (c) absorption spectrum changes of ABDA (20 μM) in the presence of Py-Cage NPs in H_2O under the irradiation (20 mW·cm^{-2}) with different duration; (d and e) the $^1O_2$ production of Py-Cage and Py-Cage NPs under white light irradiation (20 mW·cm^{-2}) using ABDA as an indicator; (f) the PL spectrum changes of DHR123 (20 μM) in the presence of Py-Cage NPs (10 μg/mL) upon light irradiation (20 mW·cm^{-2}) in H_2O; (g) The $\cdot O_2^-$ production of Py-Cage, Py-Cage NPs (10 μg/mL) under white light irradiation (white light, 20 mW·cm^{-2}) using DHR123 as an indicator; (h) the PL spectrum changes of HPF (20 μM) in the presence of Py-Cage NPs (10 μg/mL) upon light irradiation (20 mW·cm^{-2}) in H_2O; (i) the ·OH production of Py-Cage, Py-Cage NPs (10 μg/mL) under white light irradiation (white light, 20 mW·cm^{-2}) using HPF as an indicator.

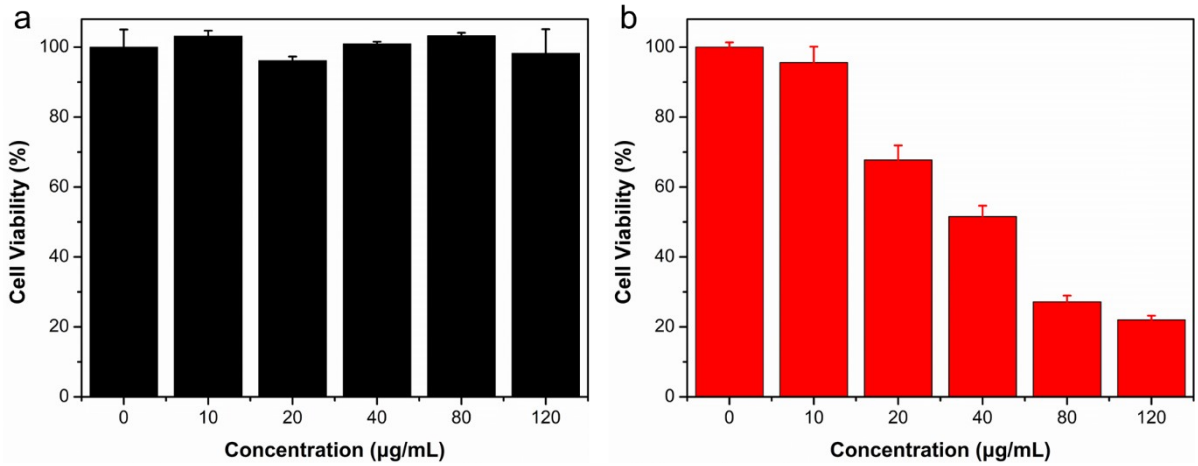

Figure S31. Cell viabilities of 4T1 cells receiving different concentrations of Py-Cage NPs under (a) dark and (b) light conditions (80 mW·cm^{-2}, 15 min).

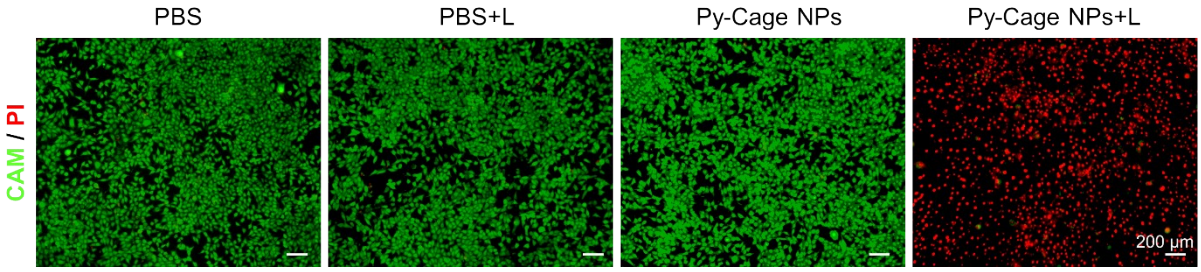

Figure S32. Live/dead cell staining of 4T1 cells after different treatments, live cells were stained green by CAM and dead cells were stained red by PI. Scale bar = 200 μm.

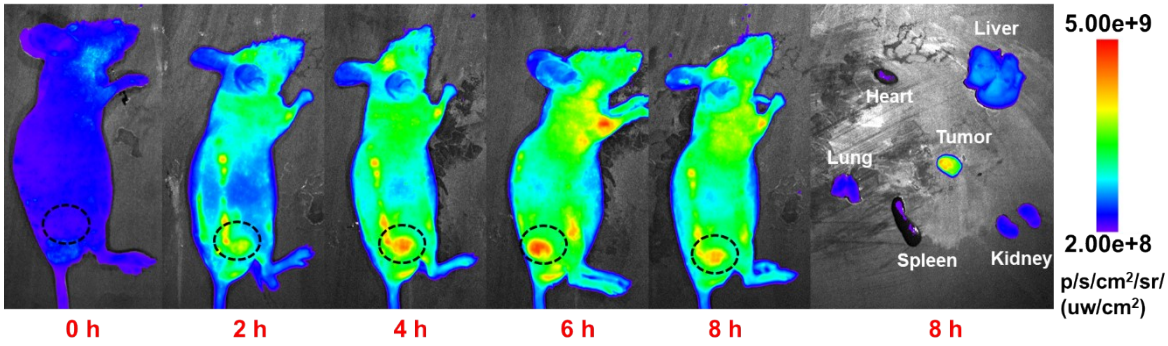

Figure S33. Fluorescence images of tumor bearing mice at different times after intravenous injection of Py-Cage NPs (300 μg/mL, 100 μL/mouse) via tail vein.